VII МЕЖДУНАРОДНЫЙ СИМПОЗИУМ
ПО УДАРНЫМ ТРУБАМ

препринт 307

Р.И.Солоухин

МЕТОДЫ ИЗМЕРЕНИЙ И ОСНОВНЫЕ РЕЗУЛЬТАТЫ В ЭКСПЕРИМЕНТАХ НА УДАРНЫХ ТРУБАХ

НОВОСИБИРСК
1969

A B S T R A C T

The full exploitation of shock tube techniques in chemical physics research strongly depends on the development of a variety of specific procedures for the rapid measurement of the temporal shocked gas thermodynamic parameters in a nonequilibrium zone, e.g. the temperature of density. The sensitivity of the method utilized, the response time, the range of applications, and the extent of interference with the phenomena under study should be considered in comparing varlous available techniques of measurement. Each of the methods should be characterized also with respect to the adequate and suitable choice of the gas parameters to be effectively detected in a shock tube flow. In this paper, some of the recently developed experimental techniques for obtaining fundamental shock tube data have been summarized in the following particular aspects:

1. Evaluations of the limits of variation of pressures, temperatures and densities in relaxation zones. Hydrodynamic effects of chemical reactions in simplest shock tube flows.

2. Advances in rapid photography and instrumentation. Laser techniques and compensating methods. Electronics and detectors of the high time resolution.

3. Gas temperature measurements. Spectoscopic techniques, recent developments, and summary data. Hydrodynamic methods. Plasma physics experiments. X - ray spectroscopy, Doppler broadening at high temperatures. Laser scattering technique.

4. Gas density measurements I. Brief review on advances in quantitative schlieren and interferometer methods. Interferometer - chronometers. Laser - interferometers. Microwave reflection technique.

5. Gas density measurements II. Laser beam scattering and spectral distribution of the scattered radiation.Electron, ions and neutral particles beams. Advances in UV and IR absorption techniques.

6. Conductivity measurements in shock and detonation waves. Coil impedance technique for reflected wave studies. Comparison with probe and microwave diagnostics..

7. Pressure measurements in complex shock tube experiments. Expansion wave technique and recombination kinetic data.

8. Shock tube experiments in exothermal systems. Ignition kinetic data. Nonstationary reaction zones and role of combined measurements. Illustrations.

9. Tables of systematics in experimental techniques. (density and temperature measurements, applications and recommendations). Tables of the basic data obtained from shock tube experiments (molecular relaxation, reaction kinetics, recombination processes).

* * *

1. INTRODUCTION

The rapid development and wide utilization of shock tube techniques have recently become an important modern physical method in das dynamics and kinetics experiments.Extremely short response times are particularly required in shock tube studies but no serious limitations have arisen in this respect in applications of laser techniques, optical spectroscopy, interferometry, scattering of light and particle beams, and ofher experimental methods with sensitivity and accuracy not worse than those in stationary measurements. Gas density and temperature measurement techniques have especially advanced during the last years. Simultaneous determination of the concentration of chemical species as a function of time seems to be the most important diagnostic technique in shock tube kinetic studies together with the measurement of the gross variables in the experiment.

As an introduction to the Shock Tube Symposium session, this survey will cover only a few specific topics in shock tube operations and present some illustrations of several experimental methods. More detailed reviews and particular discussions are already available [1- 7], though certain features of novel techniques and their relations to neighbouring plasma physics experimental methods should be considered in more detail in order to emphasize an extension of these methods to new ranges of gas parameters and better time resolutions.

In a shocked gas, the total change of a gas parameter in

a nonequilibrium zone behind a shock front essentially depends on the amount of the absorbed or released energy. Therefore, a choice of a suitable variable to be determined behind shock waves is of particular interest to the method of measurement. For example, it is easy to show that pressure measurement cannot be the suitable method in vibrational relaxation studies because the pressure deviations are very small compared to density or temperature changes whereas in detonations and in exothermal reactions determination of pressure appears to be quite effective and appropriate.

To evaluate the pressure and density variations in a relaxation zone, a strong shock approximation can be considered:

$$\frac{2Q}{V_s^2} = (1 - \frac{\rho}{\rho_1})\,(\frac{\gamma + 1}{\gamma - 1}\frac{\rho_1}{\rho} - 1)$$

Close to the shock front, pressure and density change in a reaction zone can be estimated as

$$\frac{\Delta p}{p} = -\frac{\rho_1}{\rho}\frac{\Delta Q}{\varepsilon} \qquad \frac{\Delta \rho}{\rho} = -\frac{2}{\gamma + 1}\frac{\Delta Q}{\varepsilon}$$

where ΔQ is the energy released (or absorbed) and ε is the internal energy of the shocked gas. Thus, for vibrational relaxation in a diatomic gas $\Delta\rho/\rho \sim 0.3$ whereas $\Delta p/p \sim 0.05$ only. The same proportions would be valid in highly diluted exothermal systems ignited behind incident shock waves though in detonation regimes both pressure and density variations across the reaction zone appear to be quite significant. It should be noted however that a thermodynamic gas state behind an incident shock wave propagating in a gas system of small ΔQ closely

corresponds to isobar conditions.

As an example, typical simultaneous registrations of the density and pressure variations within an induction zone behind a shock wave propagated in oxy - hydrogen mixture diluted with argon are shown in Fig. 1. The density change is quite remarkable in the interferogram whereas the pressure fall in the course of the reaction is negligible [6].

Generally, the extent of a change of the measured variable in the course of the process under study should be considered in comparing various experimental methods together with their time resolution, sensitivity, range of applications, reproducibility and accuracy, ets. A comparison with plasma physics methods seems to be quite instructive bearing in mind the similar purposes of these methods and their possible applications to shock tube studies at moderate temperatures.

2. ADVANCES IN RAPID PHOTOGRAPHY AND INSTRUMENTATIONS

Different methods for rapid photography, oscillography, and fast electronics are available for shock tube studies. But significant and noteworthy improvements of these methods as well as new advances have been developed in a number of recent experimental works. The use of a pulsed solid - state laser as a light source in high speed stroboscopic photography made it possible to obtain very clean schlieren records and interferograms [8-12] with exposures of 10^{-8} sec and with an interval between flashes of 10^{-6}sec . Monochromatic laser light illuminator is of particular importance for interferometer methods and it may be nicely synchronized with the process investigated

using a Kerr - cell in Q - spoiled laser generation regimes. A laser light pulse may be used also as a spark gap trigger with a response time of 10^{-8}sec [12].

A simple technique which uses an ordinary flash lamp as a light source still seems to be quite advantageous in obtaining the "frame" photographs of quasi - stationary shock tube flows in a compensating registration regime [6,13]. The process which is visualized by some standard methods is recorded by a streak camera through a narrow slit placed normal to the direction of movement, providing that the film velocity is equal to the image velocity of the process. A typical record of a shock tube flow is shown in Fig. 2. Quite lengthy gas flow patterns might be registered using this technique and only narrow wall windows are required in the observation chamber.

An ordinary framing camera should be recommended for use in studies of quasi-stationary two-dimensional shock tube flows because it is possible to select a suitable stationary stage of the process. As an example, a series of interferograms of the shock wave expansion flow of dissociated oxygen obtained by a zero-fringe interferometer [14] is shown in Fig. 3. Constant density lines in the interferogram are used for a time resolved measurement of the density field distributions in this non-steady supersonic flow.

Spark photography was shown to be useful in ballistic-type shock tube experiments [15]. Typical schlieren records of a shock wave diffracted around a cylinder are shown in Fig. 4.

Although shock velocity measurement techniques have been

widely described, a number of new advances in this field should be mentioned. Schlieren or shadow light beam detectors have been utilized [16,17]. A simple photomultiplier system might be adopted in luminous shock front registrations using a number of wall slits focused to the same p.m. cathode. Shock velocities ranging from 20 to 100 km/sec have been measured employing this technique. Microwave Doppler techniques have also been applied to shock velocity measurements [18,19]. In addition mention is made of a simple electronic trigger device [20] in which shock velocity data are utilized to provide an automatic change of the time delay.

Hall - effect methods for shocked gas velocity measurements in the presence of magnetic field have been shown to be a suitable technique in shock tube studies at moderate temperatures [21-23]. No remarkable force interactions between a gas flow and magnetic field occured in this case and electric fields of about 10 volts per cm are induced at flow velocities of 1 km/sec in a magnetic field of 10 kilogauss. In gaseous detonation studies [23] an accuracy of 2 to 4 per cent has been obtained using this technique. Precise flow velocity measurements are essential for hydrodynamic methods of gas temperature measurements which are to be discussed later.*

Various electronic scanning systems have been applied in rapid spectroscopic methods. Image converter technique has been employed in a device shown in Fig.5a, which can provide rapid scans of spectral line profiles [6]. An electron beam is transmitted through a narrow slit-diaphragm and detected

---

* It is interesting to note the flow velocity measurements by combining the Doppler principle with the schlieren method and with the use of laser light. [166]

directly by a photomultiplier system. The image of a spectral line on the cathode is converted from the cathode plane into the diaphragm plane while being magnified 10^4-10^5 times. Scanning regimes and suitable time resolutions are provided by an electrical deflection of the converted line image across the slit. Line recording times of $5 \cdot 10^{-8}$sec might be easily achieved by employing this method. Similar principles may be developed to record a spectrum line profile by scanning Fabry - Perot interferometer fringes through an annular slit.

A different method has been proposed for the same purpose on the basis of a fiber optic techniques [24], see Fig. 5b. An image of a spectrum line is focused on a number of fiber-optic guides connected with a p.m. system. The light intensity distribution is then determined using a fast electronic commutator with seven independent information channels which provide the succesive detection of light intensity p.m. signals reproducing the line profile. A system of 350 light guides was shown to be sufficient to obtain a record of a spectral interval of 0.5 Å with a time resolution less than one microsecond.

3. GAS TEMPERATURE MEASUREMENTS

Numerous techniques have been developed for gas temperature measurements in shock waves and quite detailed surveys are available now in this area [3,4,6,16]. It appears to be reasonable to restrict our consideration here only to some of the recent results in applications of line reversal and relative line intensity methods; a brief summary will be made of hydrodynamic temperature measurements as well as of plasma physics techniques applied at

high temperatures.

Spectrum-line reversal measurements behind incident shock waves have been performed successfully in various gaseous systems. Pioneering attempts made with sodium line emission and absorption measurements [3,25,26] yielded quite acceptable shocked gas temperatures in air and in nitrogen whereas the measured temperatures in argon were significantly lower than the calculated values [27,28]. The difference observed was about 600°K at T_s = 2900 °K and gas pressure of one atm [28], this result was also obtained in experiments [16] where Ba II - line reversal temperatures have been measured in argon ($\Delta T \sim 2000$°K at T_s= 6000°K). The difference vanished only at shock pressures higher than 12 atm.

This problem stimulated a number of interesting investigations on electronic excitation and radiative equilibrium of sodium atoms and barium ions in the shock-heated argon and in molecular gases [16,28]. It was suggested that collisions with argon atoms could not maintain the thermal equilibrium in the system due to their small cross-sections. Comparing measured and equilibrium temperatures one could estimate collision resonance quenching rates from the ratio of the collisional transition probability to the classical probability of radiative escape (approximately $10^8 sec^{-1}$).

The effective quenching cross-section of sodium atom--argon collisions was evaluated [28] to be lower than 10^{-19} - 10^{-20} cm^2 whereas for Ba^+ - Ar collisions $\sigma = 4 \cdot 10^{-17}$cm^2 was obtained [16]. Thus, non-equilibrium radiation will be

observed during periods of the order of $\tau \sim (n v_T \sigma)^{-1} \sim 10^{-8}$ sec ($n \sim 10^{18} cm^{-3}$) if excited levels are depopulated by spontaneous radiative transitions. Vibrationally excited molecules of oxygen or nitrogen were found to be much more effective than neutral atoms in the thermal excitation of Na in shock waves[28-30]. For example, only 0.5 - 1 per cent of nitrogen or carbon monoxide added to argon was found to be sufficient to reach equilibrium gas temperatures within a rise time of the order of vibration relaxation periods of the impurity gas molecules [28]. The effective cross-section for the excitation of Na by energy transfer from the nitrogen molecules vibrational mode was found to be greater than 10^{-15} cm² [29]. Spectrum-line reversal temperatures currently measured within a vibrational relaxation zone appear to be a quite suitable source of data on instantaneous vibrational temperatures and relaxation times in high temperature gases. In addition, nonequilibrium expansion shock tube flows have been examined using similar methods of N_2 vibrational temperature measurements in a N_2 - Ar mixture [30].

Though spectrum-line reversal technique provides an overall accuracy of 1 - 2 per cent of a measured temperature some specific difficulties and limitations exist owing to an influence of the added emissive species. In particular, long delays in the radiative material evaporation and excitation are undesirable. The utilization of chromium lines [31-33] essentially improves the method. Observations with emission bands of the shocked gas itself [34-36] made it possible to measure electronic temperatures of excited radicals (C_2, CN) with a high time resolution.*

*Note the use of infrared CO_2 bands for spectrum-line reversal measurements. [149]

Spectrum-line reversal techniques have been applied to study the temperature distributions behind reflected shock waves [37-39]. Equilibrium temperatures have been observed in nitrogen, air, oxygen and carbon dioxide in a temperature range between 1500° and 7000 °K, temperature deviations being within 10 per cent, probably, owing to boundary layer - reflected wave hydrodynamic interactions. Again, nonequilibrium temperatures have been observed in argon using the sodium line method at pressures lower than 10 atm [38] whereas equilibrium temperatures have been measured in argon containing 0.5 per cent of carbon monoxide with an accuracy of ±35° at 2500°K [39].

Measurements of relative intensities of selected lines for which transition probabilities are known provide a quite reliable method which is applicable at temperatures higher than 4000°K [1,40-46]. Hydrogen, helium, carbon, argon and other lines might be used in measurements and quite high concentrations of free electrons are reguired in order to provide equilibrium emission of the heated gas. The higher the temperature of the gas under test the larger should be the energy difference between the upper levels of lines selected for measurements in order to obtain an appropriate accuracy. The following rough estimate of the accuracy of the method can be made:

$$\frac{\Delta T}{T} = \frac{kT}{\varepsilon_2 - \varepsilon_1} \frac{\Delta X}{X}$$

where $X = I_2/I_1$ is the measured ratio of the line intensities. Therefore, vacuum ultraviolet lines have been utilized in electromagnetic shock tube experiments [47] where temperatures of 1,5-4 ev were measured in a hydrogen plasma using C IV ion

lines (419 Å and 1549 Å).

The absolute line intensity technique as well as the method based on comparison of the line intensity in relation to the continuum intensity in the same spectral region will not be discussed here since these methods have been adequately described in the literature [1,40].

Spectroscopic methods of temperature measurements are based on the thermal equilibrium of radiative species with the gas under test and mainly electron temperatures are being determined using these techniques. Therefore, an independent verification of the data obtained which might be made by "hydrodynamic" methods seems to be an important tool in shock tube experiments[45-49]. In these methods, flow Mach numbers are determined by means of detached shock distance measurements, a blunt obstacle being placed into the supersonic flow existing behind an incident shock wave. The gas (or ion) temperature is then determined from the sound velocity of the shocked gas.

As it was shown in [46], the measured temperatures coincide within the limits of experimental errors when three independent techniques are employed: the relative line intensity method, hydrodynamic measurements, and line broadening estimations. Shocked gas temperatures of 1-2 ev and initial pressures of 0.05-1 torr in air and argon have been tested in the experiments. As an example, the temperature profile behind a shock wave propagated in argon is shown in Fig.6. The separation between thermalized and dis charge (driver) plasmas is clearly detected by both spectroscopic and hydrodynamic methods in this run while mixing between these plasmas occures at lower pressures and at

higher shock Mach numbers.

New advantages in measurements of high temperatures have been developed in plasma physics experiments. Note first that measurements of the Doppler width of a spectrum line have become a quite reliable method yielding ion temperatures with an accuracy of about 10 per cent in a temperature region of 10^2 ev and densities of $10^{14} - 10^{15}$ cm^{-3}. The half - width of a line is $\frac{\Delta\lambda}{\lambda} = 7.16\times10^{-7}(\frac{T}{\mu})^{\frac{1}{2}}$ where μ is the atomic weight and temperature is in ^oK, therefore, $\Delta\lambda$ might be a few Å at temperatures of 10^2ev. This method is restricted to moderate densities $\leq 10^{14} cm^{-3}$ because of Stark effect at higher densities.

At temperatures higher than 100 ev the technique of soft X - ray spectroscopy (2-50 Å) are particularly valuable[1,50,51]. Special crystal spectroscopy techniques and detectors have been developed in these experiments. Continuum soft X-ray emission records have also been used for plasma temperature measurements. Electron temperatures of laser [52] and theta-pinch [53,54] plasmas have been derived from relative intensities of X-ray flux transmitted through a number of metal foils of different thicknesses.

The time delay between the onset of simple kinetic processes (ionizations, nuclear reactions, etc) which occur at high temperatures with different temperature dependent sross-sections can be employed in plasma temperature evaluations [55]. Time delays in the appearance of impurity lines emission in various stages of carbon and oxygen ionization as well as relative rates of proton and neutron production in deuterium and helium - 3 plasmas have been used in these measurements which also require

knowledge of the plasma density.

Scattering of a ruby laser beam from plasmas and spectroscopic analysis of scattered light has proved to be an extre - mely effective method for measurements of ion and electron temperatures and densities [56-62], see summary in Ref. 7 . The spectral distribution of the scattered light is a function of the parameter $\alpha = \frac{\lambda}{\lambda_D^0} (4\pi \operatorname{Sin} \frac{\theta}{2})^{-1}$ where λ_D is the Debye length, θ is the angle of observation. For $\alpha \ll 1$ the electron temperature may be determined from a line width of Thomson scattering spectrum (electron Doppler broadening) whereas the ion temperature distribution is mainly reflected by the scattered radiation spectrum in a case $\alpha > 1$. A pair of line satellites displaced from the wavelength of the incident beam by plasma frequency appears in the latter case owing to the collective effect of ions and electrons, see Fig. 7. The distance of these lines from the ion mode is determined by longitudinal plasma fluctuations:

$$\Delta\lambda = \frac{\lambda_0}{2\pi c} \left[\omega_p^2 + \frac{3kT_e}{m_e} \left(\frac{4\pi}{\lambda_0} \operatorname{Sin} \frac{\theta}{2}\right)^2\right]^{\frac{1}{2}}$$

where ω_p is the plasma frequency. The shape of the central ion line of the scattered spectrum yields information on the difference between the electron and ion temperatures [56].

When considering laser beam scattering methods one should take into account the low cross - sections of the Thomson light scattering, $\sigma_T = \frac{8\pi}{3} \left(\frac{e^2}{mc^2}\right)^2 = 6.7 \times 10^{-25} \mathrm{cm}^2$, which requires both very high light intensity and high detection sensitivity (10^{-15} - 10^{-10} of the incident beam radiation). Nevertheless,

Q - spoiled laser techniques have made it possible to obtain satisfactory results from this method with a responce time of the order of 10^{-8} sec.

Multichannel registration recording systems or scanning monochromators are usually used to resolve a scattered radiation spectrum [56,62]. The use of an image converter camera [59] with an electronic shutter (10-20 nsec) and multistage light amplification made it possible to obtain a suitable photographic film image of the relevant spectral region. From accurate quantitative measurements of the exposed film quite precise information on the line profiles was cbtained.

4. GAS DENSITY MEASUREMENTS I (WAVE OPTICS)

Schlieren and interferometer techniques have been widely applied to density measurements in gasdynamics and plasma physics research. Though interferometer methods seem to be preferable in quantitative investigations, a brief summary of quantitative schlieren techniques developed in shock tube studies should be given.[6,63-66] The use of a suitable light source in a schlieren system (flash lamp, laser, etc.) and elimination of the self - luminosity of the process make possible photomultiplier measurements of the intensity of light passing a knife edge which yield information on the density gradient distribution behind a shock front. The sensitivity of the method may be increased by using a gas laser light source and by placind the knife edge a long distance from the object (in one case 7 m [65]). Detection sensitivities of about

$dn_a/dx \sim 10^{17} cm^{-4}$ and a time resolution of 0.2 μsec have been achieved in these experiments.

The density ratio across a shock front can be determined from measurements of the refraction of a schlieren light beam by the shock front if the angle between the light beam and the wave front is acute. [64] For example, the oscilloscope record of the schlieren light output is shown in Fig. 8 where density jumps were detected for incident and reflected shock waves in air.

Detection sensitivities of quantitative schlieren methods may be evaluated as follows:

$$\varepsilon = L \frac{dn}{dx} = \begin{cases} - L \frac{d}{dx} (4.46 \times 10^{14} \lambda n_e) & \text{(plasma)} \\ + L \frac{d}{dx} (3 \times 10^{-4} n_a) & \text{(neutral gas)} \end{cases}$$

where ε is a total angle of the beam deflection and L is extent of an object. For suitable conditions particle density gradients of 10^{18} and $10^{17} cm^{-4}$, respectively, for electrons or neutral atoms and molecules may be detected.

Many applications of optical interferometry to shock tubes and plasma studies have been reviewed by R.A. Alpher and D.R. White. [1] Therefore, only some of recent results should be mentioned here. The double frequency technique [67] was improved by use of a Q - spoiled ruby laser to make simultaneous measurements at both the fundamental wavelength 6943 Å and its second harmonic 3472 Å which was generated by passing the beam through a nonlinear optical medium (KDP or ADP crys -

tals). This technique which was developed for laser - induced spark interferometry [11] has been applied to shock tube studies of ionization relaxation in hydrogen. [68]

A general note might be made on the use of the zero-fringe interferometer technique. Constant density lines yield very useful information on two-dimensional density field distributions and it should be noted that the zero-fringe record is more easily interpeted than the parallel - fringe record. As a sample, two streak interferograms of the same detonation expansion process in a shock tube are shown in Fig. 9. The zero-fringe interferogram technique has also been applied to measure the gas density distribution in quasi-stationary shock tube flows of recombining gases [14], see Fig. 3.

Complete three-dimensional records of the interference pattern with complicated geometry have been obtained by means of the laser holographic technique [69,70]. Interferograms are reconstructed from a hologram which is made by means of a double exposure on the same photographic plate using a pulsed ruby laser (time-lapse interferometry), the first exposure being made with the subject absent. The resulting interferogram look quite similar to zero-fringe records and permit post-exposure examinations of the flow patterns from various directions of observation.

The increasing availability of laser techniques has stimulated the wide use of optical interferometer-chronometer arrangements. The shock tube (or other object to be studied) is placed in the optical path of an interferometer which is

illuminated with monochromatic (laser) light and the rapid shifts of parallel fringes are detected by a photomultiplier. Quite small fringe shifts may be recorded because of the high monochromaticity of laser light which also minimizes the effects of self-luminosity of the test gas or plasma [14,71]. This technigue provides electrical signals which are quite convenient since the changes in other gas parameters may be recorded simultaneously using a multiple beam oscilloscope. A typical record of the pressure and density change in an expanding sample of a dissociated gas heated by a reflected wave is shown in Fig. 10. This technique has been used in experiments on direct measurements of oxygen-atom recombination rates [14] where a partial reflection of the shock tube flow provided an expansion regime similar to that provided by single pulse shock tube techniques.

A simple evaluation of the detection sensitivity of the method can be made as follows :

$$N_f = (n-1)\frac{L}{\lambda} \sim \begin{matrix} -4.5\times10^{-14}L\lambda n_e \\ +\ 10^{-23}n_a L/\lambda \end{matrix} \quad \text{or} \quad \begin{matrix} n_e \sim 10^{15}\,cm^{-3} \\ n_a \sim 10^{16}\,cm^{-3} \end{matrix}$$

where N_f is a number of shifted fringes, $\lambda \sim 5\cdot10^{-5}$ cm, $L \sim 10$cm, n_a and n_e are respectively neutral gas particle and electron densities, and the accuracy of determining of the fringe shifts is $2\cdot10^{-2}$. A Q - spoiled CO_2 infrared laser [72] seems to be suitable for this technique since electron densities higher than 10^{14} cm^{-3} can be measured using a wavelength of 10 microns.

In recent years there have been a number of laser-interferometer studies of the electron density behaviour in ionizing shock waves and discharge plasmas.[7,73-76] A scheme which utilizes three mirrors was shown to be very promising, see Fig.11. A helium-neon laser is utilized in a two wavelength regime in which the intensities of the 0.63 and 3.39 microns laser beams are coupled and the first beam is used to follow interference in the infrared. Interference occurs between the beam reflected from M_3 and the optical cavity oscillations in the M_2- M_3 region, and modulation in the 3.39 microns laser beam intensity produces a supplementary modulation in the 0.63 μ beam radiation.* Thus intensity modulation of the output beam of the laser itself is used to detect the fringe shifts arising because of time variations of indices of refraction of a gas under investigation. The time resolution of this method was found to be limited to $3\cdot10^6$ fringes per second and electron densities of $3\cdot10^{16}$ cm^{-4} have been measured. The sensitivity of the interferometer has been improved by using a spherical mirror for M_3 rather than a planar mirror [73] and also employing a multipass mirror system which increases the sensitivity by at least a factor of 20 [73].

Faraday rotation of polarized laser radiation in a plasma which has a superimposed axial magnetic field, was used to measure the line integral of the electron density along some axial path in a theta-pinch. [77-79] The angle of rotation of the

---

* Infrared radiation has been directly monitored by using the three mirror scheme in shock tube experiments [76] with the variations in the red beam (0.63 μ) usually being recorded.

plane of polarization is $\pi \frac{\omega_p^2 \omega_H L}{\omega^3 \lambda} = 2.6\times10^{-17} H L \lambda^2 n_e$, therefore, the infrared region of the spectrum is used to measure electron densities of $10^{16} cm^{-3}$. Far infrared technique [80] seems to be promising at lower densities measurements.

Generally, electron densities in the range from 10^{14} to $10^{15} cm^{-3}$ are not easily accessible to suitable measuring techniques since this region lies below the range of the optical spectroscopy or interferometry and above the useful range of microwave systems. Even with 3 mm wave the maximum measurable density is of $10^{14} cm^{-3}$. Nevertheless, a microwave reflection method has been developed [81,82] to measure electron densities whose plasma frequency exceeds the probing one. In this method, the electron density is determined from the phase angle of the reflection coefficient at the sharp boundary of the plasma, for example, at the end of a shock tube .[82] Electron densities up to 10^{16} cm^{-3} have been measured using this technique though a discrepancy of one order of magnitude was observed compared to calculated equilibrium data on shock wave electron concentrations.

5. GAS DENSITY MEASUREMENTS II (RADIATION SCATTERING, EMISSION, AND ABSORPTION TECHNIQUES)

Laser beam scattering techniques have been utilized to measure the neutral gas densities and electron concentrations in dense plasmas by means of measurements of absolute intensities of the scattered radiation.[56-62] Rayleigh scattering from molecular gases whose cross-section is known was found to be a suitable standard of calibration for the method. Thomson

scattering computations for various laboratory plasmas have also been presented.[60] Density measurements of shock tube or laser produced plasmas of 10^{16} -10^{17} cm^{-3} have been carried out in detail with a time resolution of 10^{-7} sec. It is possible to obtain additional information on electron concentrations from spectral characteristics of the scattered radiation as it was mentioned earlier.

Electron beam transmission techniques have been widely applied for neutral gas density measurements in the range of 10^{17}-10^{18} cm^{-3} in shock tube studies. [83-85] The exponential attenuation of a beam due to electron elastic scattering, excitation and ionization processes yield accurate gas density profiles behind shock waves. Electron guns with energies of 10^4-10^5 ev and appropriate scintillator and photomultiplier systems are employed to measure instantaneous beam attenuation coefficients.

A rough evaluation of the appropriate range of the beam absorption technique applications can be made using the following approximation for cross-sections of ionization and electron impact excitation processes at energies higher than 10^3 ev: $\sigma_{i,e} \cong A/\varepsilon$, where the beam energy ε is in electron volts and A is in a range of $(1\text{-}5)\cdot10^{-14}$ for the simplest atomic and molecular gases. Thus, the absorption coefficient of the beam attenuation at pressure of 1 torr and beam energy of 10^4 ev is about $n\sigma \sim 0.1 cm^{-1}$.

The large angle (Rutherford) scattering of an electron beam has also been employed to investigate shock front structure in rarefied systems at initial pressures lower than 10^{-1} torr

in order to measure density profiles within the viscous or molecular relaxation transient zone.[86] The beam absorption technique is not applicable at these densities because only a small fraction of the beam is absorbed.

The transmission of ion and neutral particle beam across a shock tube can be also applied to density measurements in gases and plasmas.[1,6,87-89] Magnetized plasmas are particularly suitable since any changes in the electric charge of the neutral beam may be easily detected due to the effect of the magnetic field on charged particle trajectories. Three types of particle interactions appear to determine the value of the atomic beam absorption coefficients, namely, elastic scatte - ring, ionization of a gas, and charge transfer between a positive ion and a neutral atom followed by any kind of deflection in electric and magnetic fields.

Cross-sections for elastic scattering of neutral particles have been measured,[90] for example, for $H_e - H_2$ the follo - wing approximation may be used at energies of 0.5-1.9 kev: $\log \sigma = - 0.329 \log \varepsilon + 1.896$, where σ is in 10^{-16} cm^2, and ε is in ev. Thus the scattering cross-sections are of the order of 5.10^{-17} cm^2 at energies of 10^4 ev. Ionization cross--sections at beam energies of 10^4 ev and $T_e \sim 10^2$ ev appear to be lower than 10^{-16} cm^2. Quite large cross-sections are observed for the resonant charge exchange process in which the cnarge transfer between a positive ion and an atom of equal nuclear charge results in no change in the electronic state. Cross-sections for symmetric resonant charge transfer between protons and atomic hydrogen vary almost linearly from $2 \cdot 10^{-16}$

to $36 \cdot 10^{-16}$cm^2 on a semi-logarithmic scale of energies between 100 kev and 10 ev respectively.[91] At energies of 10 kev, cross-sections are 10^{-15} or $7 \cdot 10^{-16}$cm^2, respectively, for change exchange between hydrogen atom and H^+ or O^+. Provided that only neutral beam particles which have passed through the sample under test are detected, an absorption coefficient of 0.1 cm^{-1} will correspond to plasma densities of 10^{14} cm^{-3} at beam energies of 10 kev. Plasma and neutral gas densities of 10^{15} - 10^{16} cm^{-3} can be determined on the basis of the ioni- zation energy losses of a particle or ion beam provided that it is not affected by deflecting fields.

An apparatus for neutral atomic beam density measure - ments[89,92] is shown schematically in Fig.12. A multicomponent ion beam which may consist of light particles (H_2^+, He^+, H^+, Li^+) is transformed into neutral particles beam using a gas target for the charge transfer neutralization. The neutral beam which has traversed the plasma is detected by means of separate mass- -spectrometry of the different ions obtained after the partial recharging of the neutral beam in a "strip-chamber". Elect- rostatic cleaning of the beam is used twice, before and af- ter the beam passes through the plasma. A typical record of H^0- absorption when a beam passed through a discharge plasma of 10^{14}cm^{-3} density is shown in Fig.13. The He-beam attenuation profile is recorded simultaneously. He-beam absorption coef- ficients yield additional information on plasma electron tempe- ratures due to the temperature dependence of the electron impact ionization cross-sections of helium atoms (10^{-16}cm^2).

Near-uv and vacuum-uv light emission and absorption

techniques are very significant diagnostic methods in shock tube studies of vibrational relaxation, dissociation and ionization kinetics in oxygen, nitrogen, air, carbon dioxide and other systems. As it is summarized in Fig.14, the molecular bands have large photo-absorption cross-sections in this spectral region since electronic excitations are involved, as for example, in the Schumann-Runge band of molecular oxygen. [4,93-98] Note that the vacuum ultraviolet absorption coefficients at 1470 Å are decreased at high temperatures while in the "quartz" region at 2245 Å only temperatures higher than 1500°K are accessible for measurements since the vibrationally excited molecules are responsible for the light absorption in this region. This techniques allow the use of quite low gas densities in the range of 10^{16} to $10^{18} cm^3$. It is necessary to slow down the relaxation processes to improve a time resolution of the method. The detailed studies of the vibrational relaxation times of oxygen molecules [93,100] as well as dissociation rates of oxygen [93-96] and nitrogen [101] have been carried out using uv absorption techniques over the temperature range between 1500 and 20 000 °K.

The absorption oscillator strength for the hydroxyl electronic band system at 3050-3150 Å has been evaluated [102] by using measurements of the dissociation of H_2O vapours behind reflected shock waves. In the course of the wave reflection, the linear rate of increase of the absolute spectral intensity observed axially in the increasing transparent gas region was detected by monitoring the uv emission of the shocked gas layer at the end of the shock tube. From the absolute intensity data the oscillator strength (f -number) was found to be $(3.9 \pm 0.9) \cdot 10^{-3}$.

Ultraviolet emission techniques have been used for equilibrium radiation measurements in air at temperatures of 8000 - 14000°K. [103] A tungsten photoelectric cell has been used to make photometric measurements at wavelengths shorter than 2000 Å in incident shock waves. Equilibrium air radiation measurements have been performed in a shock tube combined with a projectile gun, [104] a system in which total shock velocities of 11.3 km/sec have been achieved. This technique was applied to obtain high speed recording of a wide spectral region. As the projectile flies by in the focal plane of the light collecting mirror, the luminous shock layer acts as a moving entrance slit providing the swept spectrum in the exit slit plane. The spectral region of 3000-4000 Å has been measured for air. [104] The spectrum sweeping techniques have been also utilized to yield f - numbers for the CN violet system at high temperatures in a ballistic device. [105]

The absolute emission-intensity in the wavelength range between 2300 Å and 4511 Å was found to be proportional to the square of the oxygen atom concentration in shocked ozone--argon mixtures at temperatures of 2500°-3800°K. [106] As it was shown earlier [107,108] the emission intensity which is directly proportional to the oxygen atom concentration was observed in the presence of O and CO at wavelengths below 4500 Å. Thus the emission-intensity records might be employed for instantaneous measurements of concentrations of the components of shock heated gases. In addition, note the possibility of the application of the Lewis-Rayleigh afterg-

low to atom concentration measurements in shock waves. [109]

The afterglow intensity of a shocked gas or of nitrogen molecules which were predissociated by a pulsed electric discharge was found to be proportional to the rate of recombination of atoms at temperatures in the range between 7000° and 18600°K.

Emission and absorption measurements in the infra-red region of the spectrum have become important experimental methods for shock tube kinetic studies. The instantaneous rate of change of a molecular gas concentration behind a shock front can be reliably derived from emission or absorption profiles obtained by the use of a rapid response time infrared detector. Some of the specific shock tube instrumentations for the infra-red studies have been described. [2] The possibility of using liquid-nitrogen cooled gold-doped germanium or In Sb photo - conductive detectors should be particularly mentioned.

As an example, two records of the infrared emission around 4.5 microns from a shocked N_2O - Ar mixture are shown in Fig.15. The emission is fairly constant in the equilibrium vibrational temperature region at rather low temperatures whereas a drop is seen at higher temperatures due to a relaxation process of the N_2O thermal decomposition. Thus both the vibration relaxation times (the emission rise time), and decomposition rates can be determined from the ir emission records. Infra red light absorption records in pure N_2O (Fig.15 c) show a behaviour similar to that of the shocked gas system. Ba F_2 infrared optics have been employed in these experiment together with a gold-doped germanium ir detector.

The infrared emission yields a direct measurement of the instantaneous vibrational energy of a shocked gas in the case of an optically thin molecular gas system. [86] Carbon monoxide and CO_2 vibration relaxation times as well as CO_2 and HF

dissociation rates [86,110-112] have been determined by observations of infrared emission behind incident shock waves. Water vapour absorption coefficients in the vicinity of 2.7 microns and H_2O decomposition rates have been measured in incident and reflected shock waves at high temperatures. [113,114]

In addition, ionization rates have been measured from the infrared emission of air around 6 microns. [115] Far-infrared radiation from a high-temperature air plasma was shown [103] to be predominantly that produced by free-free transitions of electrons (bremsstrahlung), therefore, the electron density behind the shock front might be determined by using this technique.

6. ELECTRICAL CONDUCTIVITY MEASUREMENTS IN SHOCK WAVES

Measurements of the electrical conductivity in a partially ionized gas can yield information on electron concentrations as well as on electron-atom collision frequencies:

$$\chi = \frac{n_e e^2}{m_e \nu_{ec}} \cong \frac{n_e e^2}{\sqrt{8\pi}\, m_e n_a \sigma_{ec} kT} \cong \frac{4\times10^{-10} n_e}{n_a \sigma_{ec} T}$$

where χ is the electrical conductivity, n_e and n_a, respectively, electron and the other particles densities, and σ_{ec} is the electron-particle collisional cross-section.

In addition to the well-known method of Lin [116] which is based upon the dynamic interaction of the shock tube flow and magnetic field, different probe techniques developed for

measurements in slightly ionized gases should be mentioned. Coil impedance and Q-factor probes have been used to measure the electric conductivity behind incident and reflected shock waves in air argon and in argon seeded with alkali metals[117-119]. The principles of the methods are based on a the reactance or resistance change of a radiofrequency tuned cirquit in the presence of a plasma sample inside or around the probe coil. A miniature conductivity probe which was calibrated in a shock tube was employed [118] in plasma jet conductivity measurements in the range of 0.1-10 $(ohm.cm)^{-1}$.

The simplest d.c. probe resistance measurements yield reasonable values for the average gas conductivity between probe and wall or for samples in a gap probe in the case of gaseous detonation studies [23,120-122], whereas the Langmuir probe technique when used in shock tube measurements [123] does not yield a meaningful voltage-current relation. Meanwhile, a double probe method with a high frequency multistep pulse voltage has been effectively applied to conductivity measurements in detonation waves. [124] In addition, some attempts to study electric conduction mechanisms between cold electrodes in a high-velocity, shock ionized air plasma at temperatures above 6000°K and electron densities of the order of 10^{14} cm^{-3} [125,126] should be mentioned.

The conductivity data obtained by the d.c. gap probe and 3 cm microwave absorption in detonation waves in $C_2H_2+O_2$ [122] are in close agreement and are seen to be slightly higher than the calculated equilibrium values. Similar results were obtai-

ned in our experiments where electron densities of 10^{12} cm^{-3} were detected in $C_2H_2+O_2$ at initial pressures 0.1 atm while using an 8 mm wavelength microwave interferometer.

Conductivity and microwave absorption measurements in shock tube flows with well-known equilibrium gas parameters may be used to determine the value of the electron collisional cross-sections at high temperatures for a variety of molecular and atomic systems. This method is very suitable for electron collision studies since purely thermal heating is employed as a plasma source, strong electric fields are absent; and electron densities are high enough to ensure equilibration by electron impacts in sufficiently short times. Effective electron-particle collisional cross-sections for the oxygen, nitrogen and other species have been determined in the temperature range between 3000° and 5000°K by employing the microwave absorption technique in shock tube experiments. [127] For example, σ_{ec} for the nitrogen molecule varies from 0.3 to $3\cdot10^{-15}cm^2$ in the range between 2800° and 5000°K.

7. PRESSURE MEASUREMENTS AND APPLICATIONS

Various methods of construction of pressure tranducers have been developed for shock tube studies and the most successful types of piezoelectric gauges now provide pressure data in complex shock tube studies with microsecond time resolutions. An accuracy of 2 - 5 per cent and detection sensitivities up to a few volts per atm have been achieved. The use of an acoustic absorbing rod with the acoustic impedance closely matched to the impedance of the sensing element was shown to be

the important detail of a device with microsecond time resolutions. [6,128-134] Barium titanate-zinc, quartz-duralumin and lead metaniobate-tin pairs seem to be the most suitable combinations.

An advantage of this design is the small size of the sensing elements, for example, piezoceramic discs 1 mm in diameter may be easily utilized without serious losses in sensitivity. We have found also that by placing the sensing element directly on the front face of an absorbing rod we avoid the stress wave dispersion arising due to coupling of longitudinal and radial elastic waves produced in the system when a step increase in pressure is applied. The rod assembly should be potted in beeswax or in silicon rubber [132] in order to provide electrical and mechanical isolation. Direct contact of the sensing element face with the shocked gas sample is very much recommended.

The role of pressure measurements is quite substantial in complex shock tube experiments since is the most appropriate dynamic characteristic to be measured with high time resolutions in complicated non-steady gas flows behind shock waves. For example, pressure records obtained in electromagnetic shock tubes [48] yielded important information on the onset of mixing between discharge and thermalized plasmas behind a shock front. Pressure measurements are particularly important in single-pulse shock tubes and in expansion wave techniques developed to study nonequilibrium processes in a shocked gas sample subjected to a negative temperature pulse. [135 137.14]

Cooling rates ranging from 10^5 to 10^6 °K/sec might be achieved in an ordinary single-pulse shock tube depending on its length. Therefore, rate constants of relatively slow processes, for example, of carbon monoxyde-atomic oxygen recombination ($k_R \sim 2 \cdot 10^{13} - 10^{14}$ cm^6 mole^{-2} sec^{-1}) have been determined using this technique. [138] Cylindrical diaphragms at the end of the shock tube have been used to get higher cooling rates in direct measurements of clorine-atom recombination rates. [139] Quite steep negative temperature pulses have been obtained using the reflected wave interaction at the contact surface provided that the reflected wave will be an expansion wave. [137] Pressure records were used in this case in order to find an appropriate wave generation regime by removing secondary compression waves.

The highest cooling rates of $(0.5\text{-}5)10^8$ °K/sec have been obtained in direct measurements of oxygen-atom recombination rates using shock tube end expansion flows [140,141] and a special expansion wave technique [14] mentioned also in [137]. Pressure traces were taken together with laser-chronometer records to follow the course of a recombination process in a cooled gas sample (Fig. 10). A summary of data on recombination rate constants derived from direct shock tube measurements in various systems is shown in Fig. 16. These data are of special interest in high temperature dissociation kinetic studies since the common method for determining the recombination rate constant from the dissociation rate constant and the equilibrium constant should be applied with caution in studes of fast processes or of complicated reacting systems.

8. SHOCK TUBE STUDIES OF EXOTHERMAL SYSTEMS

Shock tube flow patterns associated with a positive energy release might also be investigated by combining pressure measurements with schlieren or interferometer observations. Figure 17 shows typical pressure records and streak interferograms taken of the doubleheaded detonation waves proceeding into a $2CO + O_2$ mixture. The pressure profiles and density distribution fields closely correspond to each together clearly indicating the secondary compression of the shocked gas in transverse waves propagating behind a primary shock in a shock tube of square cross-section. Note the nonsteady induction zones which arose behind the curved primary shock wave; the transverse wave structure; and the behaviour of the attenuating compression "tail". The purpose of this experiment was to determine a sequence of three-dimensional wave processes occuring in spinning-type detonations in a relatively slowly-reacting system. Since single-spin and multiheaded detonation studies have been summarized in numerous survey papers and monographs, only one-dimensional shock tube flows with regular exothermal reaction zones should be considered here in order to analyze recent data on ignition kinetics in a set of complex reactive systems. In addition to studies of oxy-hydrogen [142,143] and oxy-methane [144,145] systems, shock tube ignition experiments have been carried out recently in $NH_3 - O_2$ and $N_2O - H_2$ exothermal systems. Induction period data for oxy-ammonia systems are shown in Fig. 18 [146,147] for the temperature range from 1500° to 5000°K. A typical interferogram and a hydroxyl uv emission record obtained simultaneously in a $NH_3 - O_2$

mixture diluted with argon are shown in Fig. 19 with the same time scale. The induction period and the narrow zone of heat release are clearly apparent. It is also seen that over a large range of 1/T, the activation energy of a rate-controlling reaction may be fixed at 42 kcal/mole, although different experimental techniques have been applied at low and high temperatures. It is interesting to note that the reaction rate essentially depends on N_2 and NH_3 concentrations (Fig.18).

The ignition kinetic scheme was found to be significantly different in a nitrous oxide-hydrogen system. [148] In the temperature range below 2500°K, the overall activation energy corresponds to 22 kcal/mole, while at temperatures higher than 2500°K the apparent activation energy is about 60 kcal/mole. These data have been explained in terms of a chain branched reaction mechanism in which the initiation process of the N_2O decomposition appears to be the rate-controlling stade at higher temperatures.

Infrared emission traces of N_2O around 4.5 microns taken together with OH ultraviolet emission records (Fig.20) are quite descriptive in illustrating the reaction course behind incident shock waves. If a highly diluted mixture is taken, energy deposition effects on pressure and density are negligible, thus, a classical one-dimensional reaction zone would easily be obtained. Spectroscopic measurements of selective absorption or emission appear to be more useful in these experiments than schlieren, interferometer, and pressure measurements.

9. CONCLUSIONS

In order to summarize in a brief and descriptive form the variety of procedures and available measurement techniques which have been developed recently in shock tube studies, typical methods are listed in Table I together with recommendations and ranges of appropriate applications. Some of the most important experimental data on molecular and chemical kinetics obtained in shock tube studies are presented in Table II. These systematics will not cover all the numerous basic results obtained in shock tube experiments and serve maily as illustrations of various applications of specific diagnostic techniques in nonequilibrium gasdynamics. Based on the work of the last few years, we can expect that further developments of shock tube operations and techniques of experimental measurements will lead to rapid progress in shock wave physics and chemistry.

x x x

REFERENCES

1. Huddlestone, R. H. and Leonard, S.L., (Eds.) 1965 Plasma Diagnostic Techniques, Acad. Press, N.Y. - London.
2. Bauer, S. H., Rol, N. C. and Kiefer, J. H. 1961 A Survey of the Methods for the Chemical Analysis of Transient Species with Microsecond Time Resolution, in: Physical Chemistry in Aerodynamics and Space Flight, v.3,pp.118-131.
3. Gaydon, A. G. and Hurle, I. R. 1963 The Shock Tube in High-Temperature Chemical Physics, Chapman and Hall Ltd., London.
4. Stupochenko, E. V., Losev, S. A. and Osipov, A. I. 1965 Relaxatsionnye Processy v Udarnykh Volnakh, Nauka, Moscow.
5. Strehlow, R. A. 1967 Shock Tube Chemistry Techn. Report AAE 67-2, University of Illinois, Urbana.
6. Soloukhin, R. I. 1966 Shock Waves and Detonations in Gases, Mono Book Corp., Baltimore, Maryland; Nesterikhin, Yu. E. and Soloukhin, R. I. 1967 Methody Scorostnykh Izmerenii v Gasodynamike i Fizike Plasmy, Nauka, Moscow.
7. Dushin, L. A. and Pavlichenko, O. S. 1968 Issledovanie Plasmy s Pomoshju Laserov, Atomizdat, Moscow.
8. Hecht, G. J., Steel, G. B. and Oppenheim, A. K. 1966 ISA Transactions, 5, 133.
9. Oppenheim, A. K., Urtiew, P. A. and Weinberg, F. J. 1966 Proc. Roy. Soc. A291, 279; A295, 13.
10. Krugliakov, E. P., Malinovsky, V.K. and Nesterikhin, Yu. E. 1965 Magnitnaja Hydrodynamika 1,80; 2,31.
11. Alcock, A. J, Panarella, E. and Ramsden, S. A. 1966 Proc. Sevenths Intern. Confer. Phenomena in Ionized Gases,p.224, Beograd; Appl. Phys. Letters 8, 187.
12. Panarella, E. 1966 Optical Interferometry for Plasma Measurements in a Theta-Pinch Device, Mech. Eng. Report No. MT-57, NRCC, Ottawa.

13. Soloukhin, R. I. 1967 Eleventh Symposium (International) on Combustion, p 671, The Combustion Institute, Pittsburgh, Pa.

14. Soloukhin, R. I. 1967 Combustion and Flame, 11, 489.

15. Syshikova, M. P., Bereskina, M. K. and Semenov, A. N. 1967, in: Aerofizicheskie Issledovanija Sverkhzwukovykh Techenii, p. 7, Nauka, Moscow-Leningrad.

16. Faizullov, E. S. 1962 Proc. P. N. Lebedev Phys. Institute, USSR Acad.Sciences (Moscow) 18, 105.

17. Bereskina, M. K., Dobrynin, B. M., Semenov, A. N. and Syshikova, M. P. 1967, in : Aerofizicheskie Issledovanija Sverkhzwukovykh Techenii, p. 54, Nauka, Moscow-Leningrad.

18. Brossard, J., Manson, N., Pelhate, M. and Vauthier, R. 1966 Compt. Rend. Acad. Sc. Paris B263,593; 1967 Le Journal de Physique, 28, 487.

19. Aro, T. O. and Walsh, D. 1966 Journ. Sci. Instr. 43, 572.

20. Nemkov, R. G. 1967, in: Svoistva Gasov pri Vysokikh Temperaturakh, p. 151, Nauka, Moscow.

21. Vasilieva, R. V. 1965 Zh.Prikl. Mekh. Tekhn. Fiz. 5, 127.

22. Croce, P. A. 1965 Rev. Sci. Instr. 36,1561.

23. Soloukhin, R. I. 1966 Teplofizika Vysokikh Temperatur 4, 176; see also : Veyssiere, M. and Brochet, C. 1968 Compt. Rend. Acad. Sc. Paris, B267, 924.

24. Gluskin, E. S., Savchenko, O. Ja. and Shun'ko E. V. 1968 Preprint No 226, Inst. Nucl. Phys. USSR Acad. Sci., Novosibirsk.

25. Sobolev, N. N., Potapov, A. V., Kitaevy, V. F., Faizullov, F. S., Aljamovskii, V. N., Antropov, E. T. and Isaev, I. L. 1958 Izv. Akad. Nauk SSSR (Phys. ser.) 22, 730.

26. Clouston, J. G., Gaydon, A. G. and Glass, I. I. 1958 Proc. Roy. Soc. A248, 429.

27. Clouston, J. G., Gaydon, A. G. and Hurle, I. R. 1959 Proc. Roy. Soc. A252, 143.

28. Tsuchiya, S. and Kuratani, K. 1964 Combustion and Flame, 8, 299.

29. Hurle, I. R. 1964 Journ. Chem. Phys. 41, 3911.

30. Hurle, I. R. and Russo, A. L. 1965 Journ. Chem. Phys. 43, 4434.

31. Gaydon, A. G. and Hurle, I. R. 1961 Proc. Roy. Soc. A262, 38.

32. Gaydon, A. G., Hurle, I. R. and Kimbell, G. H. 1962 Proc. Roy. Soc. A273, 291.

33. Coates, P. B. and Gaydon, A. G. 1965 Proc. Roy. Soc. A283, 18.

34. Fairbairn, A. R. 1962 Proc. Roy. Soc. A267, 88.

35. Fairbairn, A. R. 1963 Proc. Roy. Soc. A276, 513.

36 Soloukhin, R. I. and Sharapova, T. A. 1962 Zh. Prikl. Mekh. Tekhn. Fiz. 2, 37.

37. Kudryavtsev, E. M., Sobolev, N. N., Tunitskii, L. N. and Faizullov, F. S. 1962 Proc. P. N. Lebedev Phys. Inst., USSR Acad. Sciences (Moscow), 18, 159.

38. Borisov, A. A., Zaslonko, I. S. and Kogarko, S. M. 1964 Zh. Prikl. Mekh. Tekhn. Fiz. 6, 104.

39 Tsuchiya, S. and Kuratani, K. 1965 Journ. Chem. Phys. 42, 2986.

40. Griem, H. R. 1964 Plasma Spectroscopy, McGraw-Hill Book Co., Inc.

41. Barnard, A. J., Cormack, G. D. and Simpkinson, W. V. Canad. Journ. Phys. 40, 531.

42. Soloukhin, R. I. and Toktomyshev, S. D. 1965 Zh. Prikl. Mekh. Tekhn. Fiz. 5, 124.

43. Coates, P. B. and Gaydon, A. G. 1966 Proc. Roy. Soc. A293, 452.

44. Fukuda, K., Ishii, K., Okasaka, R. and Fujimoto, T. 1965 Journ. Phys. Soc. Japan, 20, 2309.

45. Soloukhin, R. I. 1966 Proc. Seventh Intern. Confer. Phenomena in Ionized Gases, p.800, Beograd.

46. Pietrzyk, Z. A., Soloukhin, R. I. and Toktomyshev, S.D. 1967 Zh Prikl. Mekh. Tekhn. Fiz. 4, 104.

47. Dolgov-Saveljev, G. G., Krugliakov E. P., Kurbatov, A. I., Malinovskii, V. K., Nesterikhin, Yu. E. and Sagdeev, R. Z. 1968, Issledovanie Structury Quasistationarnykh Udanykh Voln v Plasme, in : Annual Review, p. 14, Inst. Nucl. Phys. USSR Academy of Sciences, Novosibirsk.

48. Vorotnikova, M. I. and Soloukhin, R. I. 1964 Zh. Prikl. Mekh. Tekhn. Fiz. 5, 138.

49. Pietrzyk, Z. A. 1964 Arch. Mech. Stos. 2, 16; 1967 Fluid Dyn. Trans.(IBTP, Polish Acad. Sci.) 3, 343.

50. Sawyer, G. A., Bearden, A. J., Henins, I., Jahoda, F. C. and Ribe, F. L. 1963 Phys. Rev. 131, 1891.

51. Dolgov-Saveljev, G. G. and Panchenko, V. E. 1967 Tekhnika Issledovanija Mjagkogo Rentgenovskogo Izlutchenija Plasmy, Prepr. 175, Inst. Nucl. Phys., USSR Acad. Sciences, Novosibirsk.

52. Alcock, A. J., Pashinin, P. P. and Ramsden, S. A. 1966 Phys. Rev. Letters, 17, 528.

53. Bogen, P., Lie, Y. T., Rusbuldt, D. and Schluter, J. 1968 Paper CN-24/K-10, Third IAEA Fusion Conference, Novosibirsk.

54. Alinovskii, N. I., Nesterikhin, Yu. E., Papyrin, A. N. and Ponomarenko, A. G. 1968 Diagnostika Plasmy, v. 2, p. 137, Atomizdat, Moscow.

55. Goldman, L. M., Kilb, R. W. and Pollock, A. C. 1964 Phys. Fluids, 7, 1005; Plasma Physics (Journ. Nucl. Energy, Part C), 6, 217; Also : Prasad, A. N. and ABD EL - Karim, K. 1968 Proc. Phys. soc. 2, 1, 77.

56. Funfer, E., Kronast, B. and Kunze, H. 1963 Phys. Letters, 5, 125; 1964 Phys. Letters, 11, 42; 1966 Phys. Rev.Letters, 16, 1082; 1967 Report IPP1/70, Inst. Plasmaphysik, Garching.

57. Ascoli-Bartoli, U., Katzebstein, J. and Lovisetto, L. 1964 Bull. Amer. Phys. Soc. 9, 495; 1965 Nature, 207, 63.

58. Ramsden, S. A. and Davies, W. E. R. 1965 Bull. Amer. Phys. Soc. 10,227; 1966 IEEE Journ. Quant. Electr. 2, 267.

59. Dolgov-Saveljev, G. G., Iskol'dskii, A. M., Krougliakov,E.P. and Malinovskii, V. K. 1967 Laser and Unconventional Optics Journ. 1, 10.

60. Gerry, E. T. and Patrick, R. M. 1965 Phys. Fluids 8, 208.

61. Izawa, Ya., Yokoyama, M. and Yamanaka, C. 1966 Journ. Phys. Soc. Japan 21, 1610; 1967, ibid. 23, 1185; 1968 Japan. Journ. Appl. Phys. 7, 954.

62. Lubin, M. J., Dunn, H. S. and Friedman, W. 1968 Paper CN-24/F-8, Third IAEA Fusion Conference, Novosibirsk.

63. Resler, E. L. and Sheibe, M. 1955 Journ. Acoust. Soc. Amer. 27, 932; Ind. Eng. Chem. 47, 1182; Also: Witteman, W. J. 1961 Rev. Scient. Instr. 32, 292.

64. Soloukhin, R. I. 1965 Fizika Goreniya i Vzryva, 1, 112, see also Ref.6.

65. Kiefer, J. H. and Lutz, R. W. 1966 Journ. Chem. Phys. 44, 658; 44, 668; Phys. Fluids, 9, 1638; 1967 Eleventh Symp. (Intern.) on Combustion, p.67, The Combustion Institute, Pittsburgh, Pa.

66. Vasil'ev, L. A. and Ershov, I. V. 1964 Doklady Akad. Nauk SSSR, 157, 317.

67. Alpher, R. A. and White, D. R. 1959 Phys. Fluids, 2, 162.

68. Belozerov, A. 1968 Study of the Initial Ionization Processes in a Strong Shock Wave, UTIAS Report No. 131, Toronto.

69. Heflinger, L. O., Wuerker, R. F. and Brooks, R. E. 1966 Journ. Appl. Phys. 37, 642.

70. Tanner, L. H. 1966 Journ. Scient. Instr. 43, 878; 1967, ibid. 44, 725; 44, 1011.

71. Jones, N. R. and McChesney, M. 1964 Journ. Scient. Instr. 41, 682.

72. Miyamoto, K., Kon, S. and Morimoto, S. 1968 Japan. Journ. Appl. Phys. 7, 1304; see also: Witteman, W. J. Appl. Phys. Letters, 10, 347.

73. Ashby, D. E. T. F. and Jephcott, D. F. 1963 Appl. Phys. Letters, 3, 13; 1965 Journ. Appl. Phys. 36, 29.

74. Thomas, K. S. 1968 Phys. Fluids, 11, 1125.

75. Gerardo, J. B., Verdeyen, J. T. and Gusinow, M. A. 1963 Appl. Phys. Letters, 3, 121; 1965 Journ. Appl. Phys, 36, 2146.

76. Fontaine, B., Inglesakis, G. and Valensi, J. 1967 Compt. Rend. Acad. Sc. Paris, 265, 1230.

77. Dougal, A. A. Craig, J. F. and Gribbe, P. F. 1964 Phys. Rev. Letters 13, 156; 1966 AIAA Journ. 4, 12.

78. Jahoda, F. C., Little, E. M., Quinn, W. E., Ribe, F. L. and Sawyer, G. A. 1964 Journ. Appl. Phys. 35, 2351.

79. Gribbe, R. F., Little, E. M., Morse, R. L. and Quinn, W. E. 1968 Phys. Fluids, 11, 1221.

80. Kon, S., Yamanaka, M., Yamamoto, J. and Yoshinaga, H.: Far Infrared CN Laser, in: Annual Review, p.89, April 1966 - March 1967, Inst. Plasma Phys. Nagoya University, Japan.

81. Tsukishima, T. and Takeda, S. 1962 Journ. Appl. Phys. 33, 3290; 1965 Techn. Note 256, Nat. Bureau Stand., Washington.

82. Takeda, S. and Tsukishima, T. 1963 Journ. Phys. Soc. Japan 18, 426; 1965, ibid. 20, 1090; 1968, ibid. 25, 297.

83. Duff, R. E. 1959 Phys. Fluids, 2,207; Bull. Amer. Phys. Soc. 4,283.

84. Busygin, E. P. and Tumakaev, G. K. 1967 in: Aerofizicheskie Issledovanija Sverkhzwukovykh Techenii, p.66, Nauka, Moscow-Leningrad.

85. Lashkov, A. I. 1965 Inzhenernyi Journal 5, 1114.

86. Camac, M. 1964 Phys. Fluids, 7, 1076; Avco-Everett Reswarch Report 194, Everett, Mass.

87. Chernetskii, A. V., Zinov'ev, O. A. and Kozlov, O. V. 1965 Apparatura i Methody Plasmennykh Issledovanii, Atomizdat, Moscow.

88. Podgornyi, I. M. 1968 Lekzii po Diagnostike Plasmy, Atomizdat, Moscow.

89. Alinovskii, N. I., Alkhimov, A. P., Kornilov, V. A., Papyrin, A. N., Ponomarenko, A. G. and Rogozin, A. I. 1968 Opredelenije Parametrov Plasmy Puchkami Neutral'nykh Atomov, Prepr. 240, Inst. Nucl. Phys. USSR Acad. Sciences, Novosibirsk.

90. Admur, J. and Smith, A. L. 1968 Journ. Chem. Phys. 48,565.

91. Fite, W. L., Smith, A. C. H. and Stebbings, R. F. 1962 Proc. Roy. Soc. A268,527.

92. Alinovskii, N. I., Nesterikhin, Yu. E. and Pakhtusov, B. K. 1967 Proc. Eighth Intern Confer. Phenomena in Ionized Gases, p.515, Vienna.

93. Losev, S. A. 1958 Doklady Akad. Nauk SSSR, 120, 1291; Soviet Phys - Dokl. Vys. Shkoly, 3, 197; Losev, S. A. and Generalov, N. A. 1966 Journ. Quant. Spectrosc. Rad. Transfer, 6,101; Kuksenko, B. V. and Losev, S. A. 1969 Doklady Acad. Nauk SSSR, 185, 69; 185, 293.

94. Camac, M. 1961 Journ. Chem. Phys. 34,448; Camac, M. and Vaughan, A., ibid 34,460.

95. Wray, K. L. 1962 Journ. Chem. Phys. 37,1254; 1963, ibid. 38,1518; 1965 Tenth Symp. (Intern.) Combust., p.523, The Combustion Institute, Pittsburgh, Pa.

96. Wray, K. L. and Freeman, T. S. 1964 Journ. Chem. Phys. 40,2785.

97. Blake, A. J., Carver, J. H. and Haddad, G. N. 1966 Journ. Quant. Spectr. Rad. Transfer, 6, 451.

98. Metzger, P. H. and Cook, G. R. 1964 Journ. Quant. Spectr. Rad. Transfer, 4, 107.

99. Jacoby, Yu. A., Komin, A. V. and Ivanija, S. P. 1968 Journ. Quant. Spectr. Rad. Transfer, 8,805.

100. White, D. R. and Millikan, R. C. 1963 Journ. Chem. Phys. 39, 1803; 39,3209.

101. Appleton, J. P., Steinberg, M. and Liquornic, D. J. 1968 Journ. Chem. Phys. 48, 599.

102. Watson, R. 1964 Journ. Quant. Spectrosc. Rad. Transfer 4,1; Watson, R. and Ferguson, W. R. 1965, ibid. 5, 595.

103. Allen, R. A., Textoris, A. and Wilson, J. 1965 Journ. Quant. Spectrosc. Rad. Transfer, 5, 95.

104. Cooper, D. M. 1966 AIAA Journ. 4, 12.

105. Reis, V. H. 1964 Journ. Quant. Spectrosc. Rad. Transfer, 4,789; 1965, ibid. 5,585.

106. Myers, B. F. and Bartle, E. R. 1968 Journ. Chem. Phys. 48, 3935.

107. White, D. R. 1961 Phys. Fluids, 4, 465.

108. Myers, B. F. and Bartle, E. R. 1967 Journ. Chem.Phys. 47. 1783.

109. Wray, K. L. 1966 Journ. Chem. Phys. 44, 623.

110. Hooker, W. J. and Millikan, R. C. 1963 Journ. Chem. Phys. 38,214; Millikan, R. C. 1963, ibid. 38,2855; 1964, ibid. 40,2594.

111. Camac, M. and Feinberg, R. M. 1967, Eleventh Symp. (Intern.) p. 137, The Combustion Institute, Pittsburgh, Pa.

112. Jacobs, T. A., Giedt, R. R. and Cohen, N. 1965 Journ. Chem. Phys. 43, 3688.

113. Olschewski, H. A., Troe, J. and Wagner, H. Gg. 1967 Eleventh Symp. (Intern.) Combust. p.155, The Combustion Institute, Pittsburgh, Pa.; also: Penzias, G. J. and Maclay, G. J. 1965 Tenth Symp. (Intern.) Combust. p.189, The Combustion Institute, Pittsburgh.

114. Patch, R. W. 1965 Journ. Quant. Spectrosc. Rad. Transfer, 5, 137 .

115. Wilson, J. 1966 Phys. Fluids 9, 1913.

116. Lin, S. C., Resler, E. L. and Kantrowitz, A. 1955 Journ. Appl. Phys. 26,95; Lamb, L. and Lin, S. C. 1957, ibid. 28,754.

117. Lau, J. 1964 Canadian Journal of Physics, 42,1548; 1965, ibid. 43, 1334.

118. Stubbe, E. J. 1966 AIAA Plasmadynamic Conference, Paper 66-181, Montrey, California.

119. Poberezhskii, L. P. 1968 Teplofizika Vysokikh Temperatur, 6, 973.

120. Basu, S., Fay, J. A. 1959 Seventh Symp. (Intern.) Combust. p.277, The Combustion Institute, Butterworth, London.

121. Bellet, J. C., Brossard, J., Manson, N. and Veyssiere, M. 1964 Journ. Combust. Convers. Energies, IFCE, Paris, p. 95; Veyssiere, M. and Manson, N. 1967 Compt. Rend. Acad. Sc. Paris, 264,199; 1968, ibid. B266,990.

122. Edwards, D. H. and Lawrence, T. R. 1965 Proc. Roy. Soc. A286,415.

123. Hand, C. W. and Kistiakowsky, G. B. 1962 Journ. Chem. Phys. 6, 1154.

124. Terao, K., Nishida, Y. and Sato, T. 1967 Japan. Journ. Appl. 37,1239.

125. Hoppmann, R. F. 1968 Phys. Fluids 11, 1092.

126. Gorelova, M. A., Gorelov, V. A. and Kil'djuschova, L. A. 1969 Teplofizika Vysokikh Temperatur 7, 18.

127. Lobastov, Yu. S. 1966, in: Issledovanija po Fizicheskoy Gasodynamike, p.119, Nauka, Moscow.

128. Turetric, W. 1941 Problem der Detonation, Berlin.

129. Zaitsev, S. G. 1958 Pribory i Techn. Exper. 6,97.

130. Soloukhin, R. I. 1961 Pribory i Techn. Exper. 3,583.

131. Edwards, D. H. 1958 Journ. Scient. Instr. 35,346 i 1959 Journ. Fluid Mech. 6,497; 1962 Paper No. 109, Coll. Intern. CNRS, Gif-sur-Yvette (France); 1964 Journ. Scient. Instr.41,609.

132. Ragland, K. W. and Cullen, R. E. 1967 Rev. Scient. Instr. 38, 740 .

133. Topchian, M. E. 1962 Zh. Prikl. Mekh. Tekhn. Fiz. 4,94.

134. Guerraud, C., Leyer, J. C. and Brochet, C. 1967 Compt. Rend. Acad. Sc. Paris B264, 5; Brochet, C., Guerraud, C., Manson, N. and Veyssiere, M. 1969 ibid. B268,361

135. Glick, H. S., Klein, J. and Square, W. 1957 Journ. Chem. Phys. 27,850.

136. Wilson, J. 1963 Journ. Fluid Mech. 15,497.

137. Resler, E. L. 1966 Chemical Studies Using Gasdynamic Wave Interactions, p. 135, in: Dynamics of Fluids and Plasmas, Acad. Press Inc., New York.

138. Brabbs, T. A. and Belles, F. E. 1967 Eleventh Symp. (Intern.) on Combustion, p. 125, The Combustion Institute, Pittsburgh, Pa.

139. Jacobs, T. A., Kartunian, R. A., Giedt, R. R. and Wilkins, R. 1963 Phys. Fluids 6,972.

140. Glass, I. I. and Takano, A. 1965 Nonequilibrium Expansion Flows of Dissociated Oxygen and Ionized Argon Around a Corner, in: Progr. Aeron. Sci., ed. by Kuchemann and Sterne, v. 6, pp. 163-249, Pergamon Press; Class, I. I. 1967 Canadian Aeronautics and Space Journal, 13, 347-426.

141. Drewry, J. E. 1967 An Experimental Investigation of Nonequilibrium Corner Expansion Flows of Dissociated Oxygen, UTIAS Report No. 124, Toronto.

142. White, D. R. and Moore, G. E. 1965 Tenth Symp.(Intern.) on Combustion, p. 785, The Combustion Institute, Pittsburgh, Pa.; 1967 Eleventh Symp. (Intern.) on Combustion, p. 147, The Combustion Institute, Pittsburgh, Pa.

143. Hamilton, C. W. and Schott, G. L. 1967 Eleventh Symp. (Intern.) on Combustion, p. 635, The Combustion Institute, Pittsburgh, Pa.

144. Miyama, H. and Takeyama, T. 1965 Bull. Chem. Soc. Japan, 38, 37.

145. Voevodsky, V. V. and Soloukhin, R. I. 1965 Dokl. Akad. Nauk SSSR 161, 1118.

146. Takeyama, T. and Miyama, H. 1965 Bull. Chem. Soc. Japan, 38,1670; 1966, ibid. 39,2352; 39,2609; 1967 Eleventh Symp. (Intern.) on Combustion, p. 845, The Combustion Institute, Pittsburgh, Pa.; Miyama, H. 1968, Bull. Chem. Soc. Japan 41,1761.

147. Soloukhin, R. I. 1966 Some Shock Tube Methods in Chemical Physics, Nauka, (Siberian Division) Novosibirsk.

148. Soloukhin, R. I. and Van Tiggelen, P. J. 1969 Shock Tube Study of the Induction Lag in Nitrous Oxide-Hydrogen System, Bull. Soc. Chim. Belg. 73 (in press).

149. Galaktionov, I. I., Korovkina, T. D., Mikhalevsky, V. D. and Podmoshensky, I. V. 1969 Teplophysica Vysokikh Temperatur, 1,85.

150. Suckewer, S. 1968 Plasma Physics 10,527.

151. Elton, R. C. and Roth, N. V. 1967 Appl. Optics, 6,2071.

152. Kistiakowsky, G. B. and Kydd, P. H. 1956 Journ. Chem. Phys. 25,824.

153. Duff, R. E., Knight, H. T. and Rink, J. P. 1958 Phys. Fluids, 1,393.

154. Measures, R. M., Jaskolka, A., Rodrigo, A. B. and Pettitt, B. A. 1968 Laser Excitation Diagnostics, in: Annual Progress Report, pp. 90-93, UTIAS, Toronto.

155. Bristow, M. 1968 An Experimental Determination of the Polarizability of Singly-Ionized Argon, in: Annual Progress Report, pp. 24-25, UTIAS, Toronto.

156. Benson, S. W. and Berend, G. C. 1966 Journ. Chem. Phys. 44, 471.

157. Sutton, E. 1962 Journ. Chem. Phys. 36,2923.

158. Seery, D. J. and Bowman, C. T. 1968 Journ. Chem. Phys. 48, 4314.

159. Jones, W. M. and Davidson, N. 1962 Journ. Amer. Chem. Soc. 84, 2868.

160. Schott, G. L. and Bird, P. F. 1964 Journ. Chem. Phys. 41,2869; Getzinger, R. W. and Schott, G. L. 1965, ibid. 43,3237.

161. Hurle, I. R. 1967 Eleventh Symposium (International) on Combustion, p.86, The Combustion Institute, Pittsburgh,Pa

162. Gutman, D. and Schott, G. L. 1967 Journ. Chem. Phys.46,4576.

163. Miyama, H. and Takeyama, T. 1965 Journ. Chem. Phys. 42,2636.

164. Bull, D. C. 1968 Combustion and Flame, 12, 603.

165. Sulzmann, K. G. P., Myers, B. F. and Bartle, E. R. 1965 Journ. Chem. Phys. 42,3969; 43,1220; Brokaw, R. S. 1967 Eleventh Symposium (International) on Combustion,p.1063 The Combustion Institute, Pittsburgh, Pa.

166. Schwar, M. J. R. and Weinberg, F. J. 1969 Nature, 221,357.

TABLE I

SYSTEMATICS OF EXPERIMENTAL TECHNIQUES

Gas parameter	Measurement method	Range of applications	Detection sensitivity and accuracy, per cent	Time resolution, μ sec	Comments and recommendations	References
1	2	3	4	5	6	7
Equilibrium gas temperature	Spectrum-line reversal technique	1500°-7000°K	1-2	1-5	Nonequilibrium effects in argon at densities lower than 3.10^{19} cm^{-3}	3,4,6, 25-39,149
	Measurements of relative line intensities	4000°-40000°K	2	0.1-1	Ultraviolet region is used at high temperatures	40-47, 150
	Doppler line width	10-100 ev	10-30	1	X-ray spectroscopy of impurity lines	1,7, 50,53
	Laser cooperative scattering (ions Doppler width)	100-1000 ev	5-10	0.02-0.1	Plasma densities of 10^{16}-10^{18} cm^{-3}	53,56,58, 61,62
Electron temperature	Stark broadening of spectrum-lines	0.5-10	5-10	1	Are determined from equilibrium electron densities	1,40,46
	Laser beam (Thomson) scattering	1-10000	10-20	0.02-01	Satellite line width is measured	56,58,61
	Neutral beam absorption	20-1000	10-20	0.5-1	Temperature is determined from measurements of ionization cross-sections	1,92

1	2	3	4	5	6	7
	Soft X-ray emission technique	50-10000 ev	5-50	0.1-1	Used for evaluations	52,53, 56,151
	Radiation emitted by the succesive ionization stages	5-300 ev	25	0.1	Electron density should be known	55
Gas density	Quantitative schlieren	$5\cdot10^{14}$-10^{20} cm^{-3}	2-5	0.5-2		6,63-66
	technique (density, and density gradients)	10^{14}-10^{18} cm^{-4}	0.2-0.5	0.2-1		
	Optical interferometry	10^{16}-10^{21}	0.1-0.2	0.02-0.5		1,6,67-70
	Laser beam scattering	10^{18}-10^{21}	5-10	0.02-0.1	Rayleigh cross-sections $\sigma_R \sim 10^{-26}$ cm^2	7,58-61
	Electron beam absorption	10^{16}-$5\cdot10^{18}$	8-10	0.1		83-84
	Electron beam scattering	10^{15}-$2\cdot10^{18}$	1-5	0.5-1		85-86
	X-ray absorption	$5\cdot10^{18}$-$5\cdot10^{19}$	2-5	1-2	A noble gas is added	152,153
Mixture component concentrations	Ultraviolet and vacuum uv absorption	10^{16}-10^{19}	5-15	0.1	Absorption of O_2, N_2, CO_2, OH, NO, H_2 is employed	2,4, 93-103
	Infrared emission and absorption	$5\cdot10^{14}$-10^{20}	5-20	0.1-0.5	Systems of CO, CO_2, N_2O, NO, H_2O, NH_3, HF are recommended	2, 110-115
	Light emission in the visible; afterglow emission	10^{14}-10^{19}	5-15	1	Atomic oxygen, nitrogen, carbon monoxide	106-109

1	2	3	4	5	6	7
	Mass spectrometry	10^{18}-10^{20} (to 10^{14} in a nozzle)	0.1-1	1-10		2,137
	Laser induced fluorescence			0.1		154
Electron concentrations	Microwave techniques	10^{11}-10^{16}	0.5-5	1	Microwave reflection method is recommended at high densities	1,6,7, 81,82
	Optical interferometry	10^{15}-10^{20}	0.1-0.5	0.02-0.1	A double frequency technique is recommended	67,68,155
	Laser-interferometers	10^{14}-10^{18}	0.1-0.5	0.5-1		73-76
	Faraday rotation	10^{16}-10^{17}	1-10	1	Magnetic field is applied	77-79
	Laser beam scattering	$5\cdot10^{15}$-10^{17}	5-15	0.1	Both the satellite line width and the distance from the center are used for measurements	58,59,61
	Spectral line broadening	5.10^{15}-10^{19}	5-10	2-5		1,40,46 151
	Neutral beam absorption	10^{13}- 10^{15}	10-15	2-5	Determined from the ionsdensity	1,6,92
	Infrared emission	10^{13}-10^{16}	10-20	0.5-1	free-free transitions in ionized air	103,115

TABLE II

MOLECULAR KINETICS DATA OBTAINED FROM SHOCK TUBE EXPERIMENTS

Gas system	Kinetic process	Temperature range, °K	Measurement method	Rate constants and relaxation times	References
1	2	3	4	5	6
O_2, N_2, CO, Cl_2, Br_2, I_2, and gas mixtures (generalized,[100] to 50 per cent accuracy)	Vibrational relaxation	300-8000	Interferometer, uv-absorption, and other techniques	$p\tau_v = 10^{-8}\exp\left[1.15 \times 10^{-3}\,\mu^{\frac{1}{2}}\,\theta^{\frac{4}{3}}(T^{-\frac{1}{3}} - 0.015\mu^{\frac{1}{4}})\right]$ atm-sec where p is the pressure in atm, μ is the reduced mass of the colliding partners, $\theta = h\nu/k$ is the characteristic temperature of the oscillator.	4, 65, 93, 94, 100, 110, 156
Oxygen		1000-3700	Quantitative schlieren, uv-absorption, interferometer	$p\tau_{O_2-O_2} = (2.92\pm0.20)\times10^{-10}\exp[(126.0\pm0.9)T^{-\frac{1}{3}}]$ atm-sec	65, 93, 94, 100
		1200-10500		$p\tau_{O_2-O_2} = 3.43\times10^{-12}\exp(153T^{-\frac{1}{3}})$ atm-sec	
		300-850	Interferometer	$p\tau_{O_2-O_2} = 4.47\times10^{-9}\exp(6.3\,T^{-\frac{1}{3}})$ atm-sec	
		1000-10000	UV-absorption	$p\tau_{O_2-Ar} = 4.33\times10^{12}\exp(173.13\,T^{-\frac{1}{3}})$ atm-sec	
		1600-3300	Quantitative schlieren	$p\tau_{O_2-O} = 4.35\times10^{-8} - 7.75\times10^{-12}T$ atm-sec	65
Hydrogen		1100-2700	Quantitative schlieren	$p\tau_{H_2-H_2} = (3.9\pm0.8)\times10^{-10}\exp[(100.0\pm2.6)T^{-\frac{1}{3}}]$ atm-sec	65
				$p\tau_{H_2-Ar} = 4.1\,p\tau_{H_2-H_2}$	
Deuterium		1100-3000	Quantitative schlieren	$p\tau_{D_2-D_2} = (2.7\pm0.3)\times10^{-10}\exp[(110.5\pm1.5)T^{-\frac{1}{3}}]$ atm-sec	65
Carbon dioxide		300-5000	IR emission, electron beam scattering	$p\tau_v = 2.02\times10^{-8}\exp(36.5\,T^{-\frac{1}{3}})$ atm-sec	86
Oxygen	$O_2 + M \xrightarrow{k_D} O+O+M$	3000-7000	UV absorption	$k_{O_2-O_2} = 5.6\times10^{10}T^{\frac{1}{2}}\left(\frac{D}{RT}\right)^3\exp\left(-\frac{D}{RT}\right)$ cc/mole-sec	93
	$D = 118\ \frac{kcal}{mole}$	4200-16000		$k_{O_2-Ar} = 1.5\times10^{11}T^{\frac{1}{2}}\left(\frac{D}{RT}\right)^{\frac{3}{2}}\exp\left(-\frac{D}{RT}\right)$ cc/mole-sec	93.95
		3700-7000		$k_{O_2-N_2} = 2.5\times10^{11}T^{\frac{1}{2}}\left(\frac{D}{RT}\right)^{\frac{3}{2}}\exp\left(-\frac{D}{RT}\right)$ cc/mole-sec	93
		5000-7500		$k_{O_2-O} = 1.5\times10^{15}\left(\frac{D}{RT}\right)\exp\left(-\frac{D}{RT}\right)$ cc/mole-sec	94
		3000-10000		$k_{O_2-O_2} = [1+600\,\theta^{-2.3}\exp(-4\times10^{-9}\,\theta^{9.2})]k_{O_2-Ar}(\theta>3)$	93.95
				$k_{O_2-O} = [1+108\,\theta^{-0.58}\exp(-1.7\times10^{-3}\,\theta^{3.3})]k_{O_2-Ar}(\theta>4)$	
				where $\theta = 10^{-3}\,T^{\circ}K$	

1	2	3	4	5	6
Nitrogen	$N_2 + M \xrightarrow{k_D} N+N+M$ $D = 225 \frac{kcal}{mole}$	8000-15000	UV absorption	$k_{N_2-N_2} = (1.67\pm0.4)\times10^{17}T^{-1.6}\exp(-\frac{D}{RT})$ cc/mole-sec	101
				$k_{N_2-Ar} = (6.2\pm0.5)\times10^{16}T^{-16}\exp(-\frac{D}{RT})$ cc/mole-sec	
				$k_{N_2-N} = (7.25\pm2.7)\times10^{16}T^{-16}\exp(-\frac{D}{RT})$ cc/mole-sec	
Hydrogen	$H_2 + M \xrightarrow{k_D} H+H+M$ $D = 103.2 \frac{kcal}{mole}$			$k_{H_2-Ar} = 6.17\times10^{14}\exp(-\frac{D}{RT})$ cc/mole-sec	157
NO	$NO + M \xrightarrow{k_D} N+O+M$ $D = 150 \frac{kcal}{mole}$	3000-8000	UV absorption	$k_D = 7.0\times10^{10}T^{\frac{1}{2}}(\frac{D}{RT})^2\exp(-\frac{D}{RT})$ cc/mole-sec	95
Carbon dioxide	$CO_2+M \xrightarrow{k_D} CO+O+A$ $D = 125.7 \frac{kcal}{mole}$		UV absorption	$k_{CO_2-CO_2} = (1.5\pm0.8)\times10^{14}\exp(-\frac{87000}{RT})$ cc/mole-sec	93
		3000-5500 2800-4400	IR emission	$k_{CO_2-Ar} = [Ar]\times5.10^{14}\exp(-\frac{99000}{RT})$cc/mole-sec	113
HCl	$HCl + M \xrightarrow{k_D} H+Cl+M$ $D = 102.2 \frac{kcal}{mole}$	2900-4000	UV absorption	$k_{HCl} = 4.2\times10^{13}\exp(-\frac{81000}{RT})$ cc/mole-sec	158
HF	$HF + M \xrightarrow{k_D} H+F+M$ $D = 134.1 \frac{kcal}{mole}$	3800-5300	IR emission	$k_{HF-Ar} = (1.1\pm0.3)\times10^{19}\exp(-\frac{134100}{RT})$cc/mole-sec	112
O_3	$O_3 + M \xrightarrow{k_D} O+O_2+M$	770-910		$k_{O_3-N_2} = (5.8\pm0.6)\times10^{14}\exp(-\frac{23150}{RT})$cc/mole-sec	159

1	2	3	4	5	6
Oxygen	$O+O+M \xrightarrow{k_D} O_2 + h\nu$	3000-3700	Interferometer	$k_{O_2} = (2\div0.5)\times10^{15}$ cc²/mole²-sec	14
		1500-3000	UV absorption	$k_{Ar} \cong 2.5\times10^{13}$ cc²/mole²-sec	95
	$O+CO+M \rightarrow CO_2+M$	2800-3600	Visible light emission	$(2.6\div1.2)\times10^{13}$ cc²/mole²-sec	138
Hydrogen	$H+H+M \xrightarrow{k_R} H_2 + M$	1400-2000	UV absorption	$k_{Ar} = (4\pm2)\times10^{14}$ cc²/mole²-sec	160
		2500-7000	Spectrum-line reversal measurements	$k_{H_2} = (1.4\div3.9)\times10^{15}$ cc²/mole²-sec	161
		2500-5500		$k_H = 9\times10^{16} \div 3.7.10^{14}$ cc²/mole²-sec	161
	$H+OH+M \xrightarrow{k_R} H_2O+M$	1400-2000	UV absorption	$k_{Ar} = (4\pm2)\times10^{15}$ cc²/mole²-sec	160
	$H+O_2+M \xrightarrow{k_R} HO_2+M$	1150-1850		$k_{Ar} = 1.4\times10^{15}$ cc²/mole²-sec	160
Hydrogen-Oxygen	$H+O_2 \xrightarrow{k_1} OH+O$	1000-2000	UV absorption	$k_1 = 2.14\times10^{14}\exp(-\frac{16600}{RT})$ cc/mole-sec	143
				$k_1 = 7.76\times10^{13}\exp(-\frac{14400}{RT})$ cc/mole-sec	162
	$O+H_2 \xrightarrow{k_2} OH+H$	1000-2000	UV absorption	$k_2 = (0.4\div3.6)\times10^{13}\exp(-\frac{9200}{RT})$cc/mole-sec	143
				$k_2 = 3.24\times10^{13}\exp(-\frac{10000}{RT})$ cc/mole-sec	162
	$OH+H_2 \xrightarrow{k_3} H_2O+H$	1000-2000	UV absorption	$k_3 = (2.1\div18.9)\times10^{13}\exp(-\frac{5900}{RT})$cc/mole-sec	143
				$k_3 = 6.15\times10^{13}\exp(-\frac{5000}{RT})$ cc/mole-sec	152

1	2	3	4	5	6
	Induction times	1100-2200	Interferometer	$\tau^{-1}[O_2]^{-\frac{1}{3}}[H_2]^{-\frac{2}{3}}=2.75\times10^{13}\ \exp\left(-\frac{12200}{RT}\right)$ cc/mole-sec	142
				$\tau^{-1}[O_2]^{\frac{1}{2}}[H_2]^{-\frac{1}{2}}=0.63\times10^{13}\ \exp\left(-\frac{14200}{RT}\right)$ cc/mole-sec	142
		1000-1700	Schlieren, interferometer	$\tau^{-1}[O_2]^{-1} = 1.12\times10^{13}\ \exp\left(-\frac{19500}{RT}\right)$ cc/mole-sec	6,13
Acetylene-Oxygen	Induction times	1400-2400	Ionization measurements	$\tau^{-1}[O_2]^{-1} = 2.51\times10^{14}\ \exp\left(-\frac{14450}{RT}\right)$ cc/mole-sec	123
				$\tau^{-1}[O_2]^{-1} = 3.02\times10^{14}\ \exp\left(-\frac{17100}{RT}\right)$ cc/mole-sec	123
		1100-2200	Interferometer	$\tau^{-1}[O_2]^{-\frac{1}{3}}[C_2H_2]^{-\frac{2}{3}} = 7.6\times10^{13}\ \exp\left(-\frac{17300}{RT}\right)$ cc/mole-sec	142
	Summary data	850-2500	Various methods	$\tau^{-1}[O_2]^{-1} = 2.75\times10^{14}\ \exp\left(-\frac{23900}{RT}\right)$ cc/mole-sec	123,147, 163
Methane-Oxygen	Induction times	1200-2400	Schlieren, interferometer	$\tau^{-1}[O_2]^{-1} = 1.66\times10^{14}\ \exp\left(-\frac{33200}{RT}\right)$ cc/mole-sec	145,147
Ammonia-Oxygen	Induction times	1500-4500	Infrared emission	$\tau^{-1}[O_2]^{-1} = 1.86\times10^{14}\ \exp\left(\frac{32700}{RT}\right)$ cc/mole-sec	164
	Summary data	1400-4000	Interferometer, light emission and absorption	$\tau^{-1}[O_2]^{-1} = 3.9\times10^{14}\ \exp\left(-\frac{41200}{RT}\right)$ cc/mole-sec	146,147
Carbon monoxide-Oxygen	Induction kinetics (initiation rate constant)	1500-3000		$k_i = 3.5\times10^{12}\ \exp\left(-\frac{51000}{RT}\right)$ cc/mole-sec	165
				$k_i = 2.5\times10^{12}\ \exp\left(-\frac{48000}{RT}\right)$ cc/mole-sec	

FIGURE CAPTIONS

Fig. 1 Interferogram and pressure record of a shock wave in $0.1(H_2+O_2) + 0.9$ Ar at $p_1 = 0.1$ atm; $T_s = 1500^0$K; time marks 10 μsec apart.

Fig. 2 Interferogram of a shock tube flow made by the compensating method.

Fig. 3 Interferograms of a shock tube end expansion flow of dissociated oxygen, $M_s = 10$, $p_1 = 10$ torr, 3 μsec between frames.

Fig. 4 Schlieren frames of shock wave diffraction around a cylinder, $M_s = 2.42$, $p_1 = 200$ torr [15].

Fig. 5 a) Image converter device combined with a p.m. system for rapid recording of spectrum line profiles: (1) cathode, (2) electrode, (3) deflecting plates, (4) narrow slit, (5) a photomultiplier system;
b) Fiber optic technique for obtaining line profiles: (1) light pipes, (2)set of photomultipliers, (3) electronic commutator.

Fig. 6 Gas temperature profiles determined by different methods: (1) hydrodynamic method; (2) relative line intensity measurements, hydrogen lines; (3) equilibrium driven gas temperature; argon, $p_1 = 0.08$ torr.

Fig. 7 Laser light scattering technique: a) scattering through small angles, ion Doppler width of the central line; b) scattering through a right angle: solid line $T_e \sim T_i$, dashed line $T_e \ll T_i$.

Fig. 8 Quantitative schlieren oscillogram of the light refraction in incident and reflected shock waves in air. Pressures are recorded simultaneously.

Fig. 9 Streak interferograms of expanding detonations in $C_2H_2 + O_2$, $p_1 = 0.08$ atm: a) zero-fringe regime, b) ordinary multifringe regime.

Fig.10 Pressure (upper trace) and density (lower trace) records of the behavior of the expanding gas sample in oxygen atom recombination experiments. A scheme for producing partial reflection of the shock tube flow is also presented.

Fig.11 Schemes of the three-mirror laser-interferometers : (1) beam p.m. detector, (2) red light filter, (3) helium-neon laser tube, (4) infrared filter, (5) shock tube, (6) infrared beam detector.

Fig.12 Neutral beam diagnostic technique: (1) ion source, (2) electrode, (3) charge transfer neutralization chamber, (4,6) electrostatic cleaning plates, (5) gas sample, (7) "stripping-chamber", (8,9) masspectrometer--type beams separation device, (10) ion detection system.

Fig.13 Oscillogram showing absorption of hydrogen and helium atomic beams in a discharge in hydrogen, $p_1 = 3.10^{-3}$ torr, U = 30 kv, I = 8 ka; time marks 2 μsec apart.

Fig.14 Photo-absorption cross-sections of molecular gases in the uv region: a) temperature dependence: (1) oxygen, $\lambda = 2245$ Å, (2) carbon dioxide, $\lambda = 2380$ Å, (3) oxygen, $\lambda = 1470$ Å; b) spectral distribution of absorption coefficients: (1) oxygen, atmospheric conditions, (2) nitrogen, $T = 10000^\circ K$.

Fig.15 Infrared emission and absorption measurements, $\lambda = 4.5$ μ: a) emission $0.1\ N_2O + 0.9$ Ar, $T_s = 1150^\circ K$ b) emission, $0.1\ N_2O + 0.9$ Ar, $T_s = 1750^\circ K$, c) absorption, pure N_2O, $T_s = 1100^\circ K$.

Fig.16 Summary of data for recombination rate constants in various atomic gas systems: (1) H + H + H, (2) H + H + H_2, (3) O + O + O_2, (4) CO + O + Ar.

Fig.17 Interferograms and pressure profiles of shock tube detonations in $2CO + O_2$ at $p_1 = 0.08$ atm.

Fig.18 Summary of data on ignition delays in $NH_3 - O_2$ systems: (1) measurements in reflected waves [146], (2) our measurements, incident waves in a stoichiometric mixture diluted with argon, (3) mixture $9NH_3 + O_2$, 4 - mixture $\frac{4}{9} NH_3 + \frac{5}{9} O_2 + 10\ N_2$.

Fig.19 Oxy-ammonia ignition in a shock wave: (1) interferogram, (2) pressure, and (3) OH - emission profiles; $0.1\ (NH_3 + O_2) + 0.9$ Ar, $p_1 = 0.05$ atm.

Fig.20 Chemical reaction zone behind a shock wave in $0.03\ (N_2O + H_2) + 0.97$ Ar : (1) interferogram, (2) OH emission at 3075 Å, (3,5) pressure records, and (4) infrared emission at 4.5μ, $T_s = 1830^\circ K$, $p_1 = 0.05$ atm.

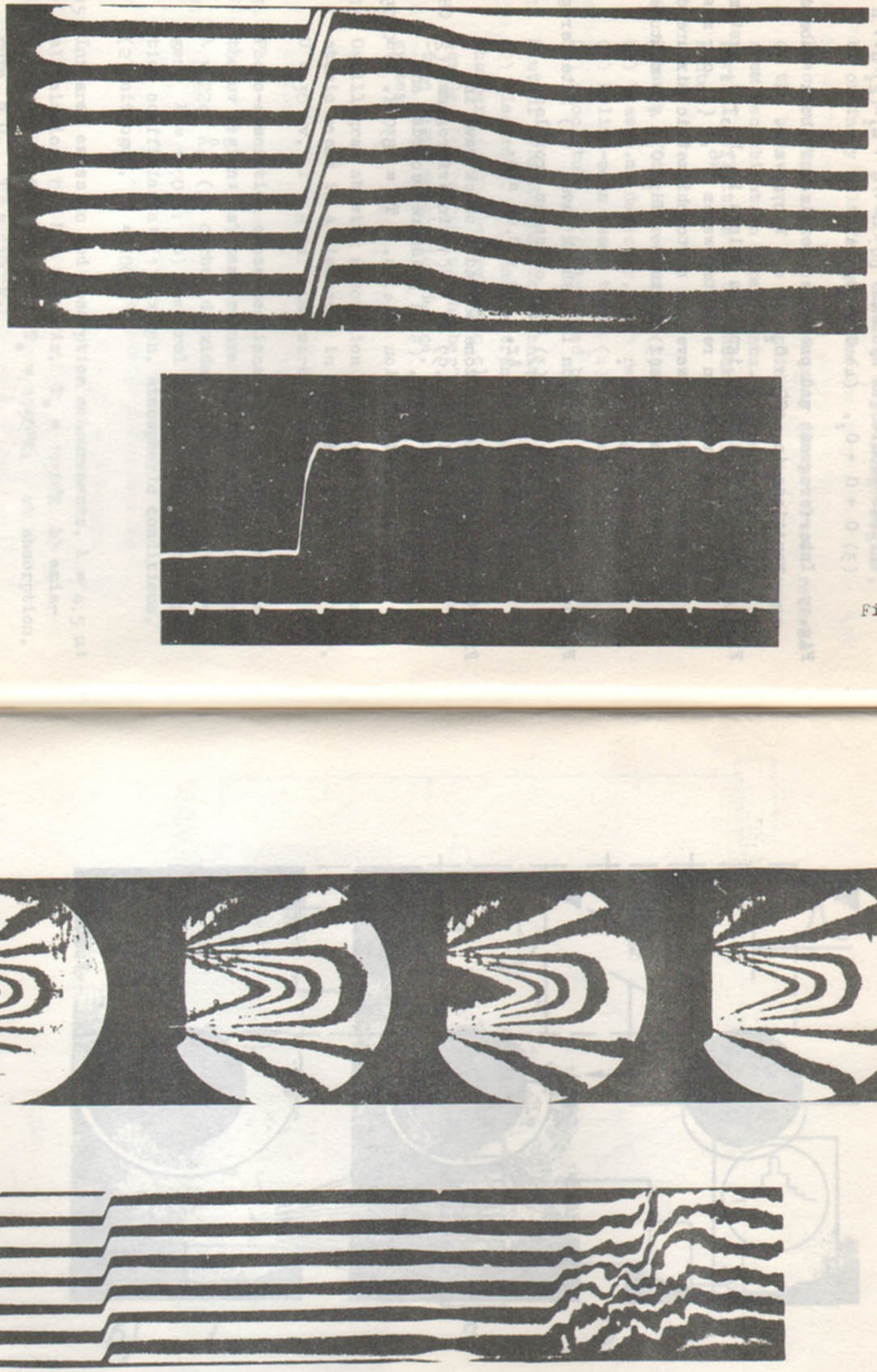

Fig.1

Fig.2

Fig.3

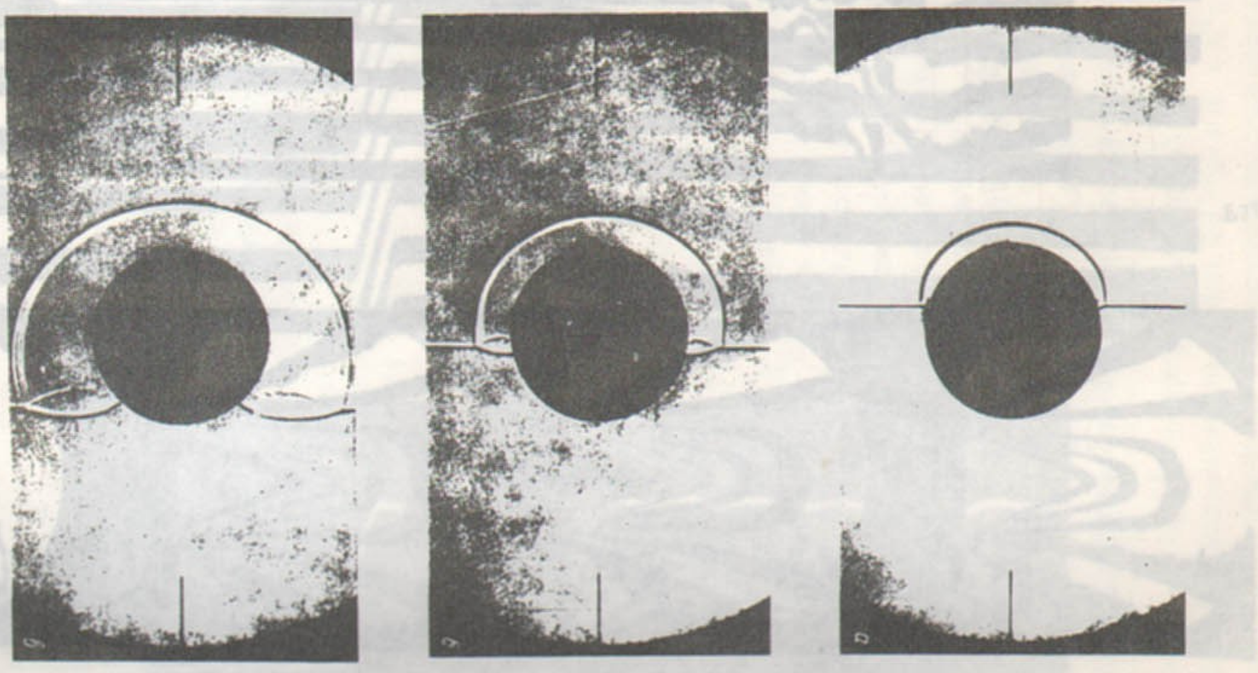

Fig.4

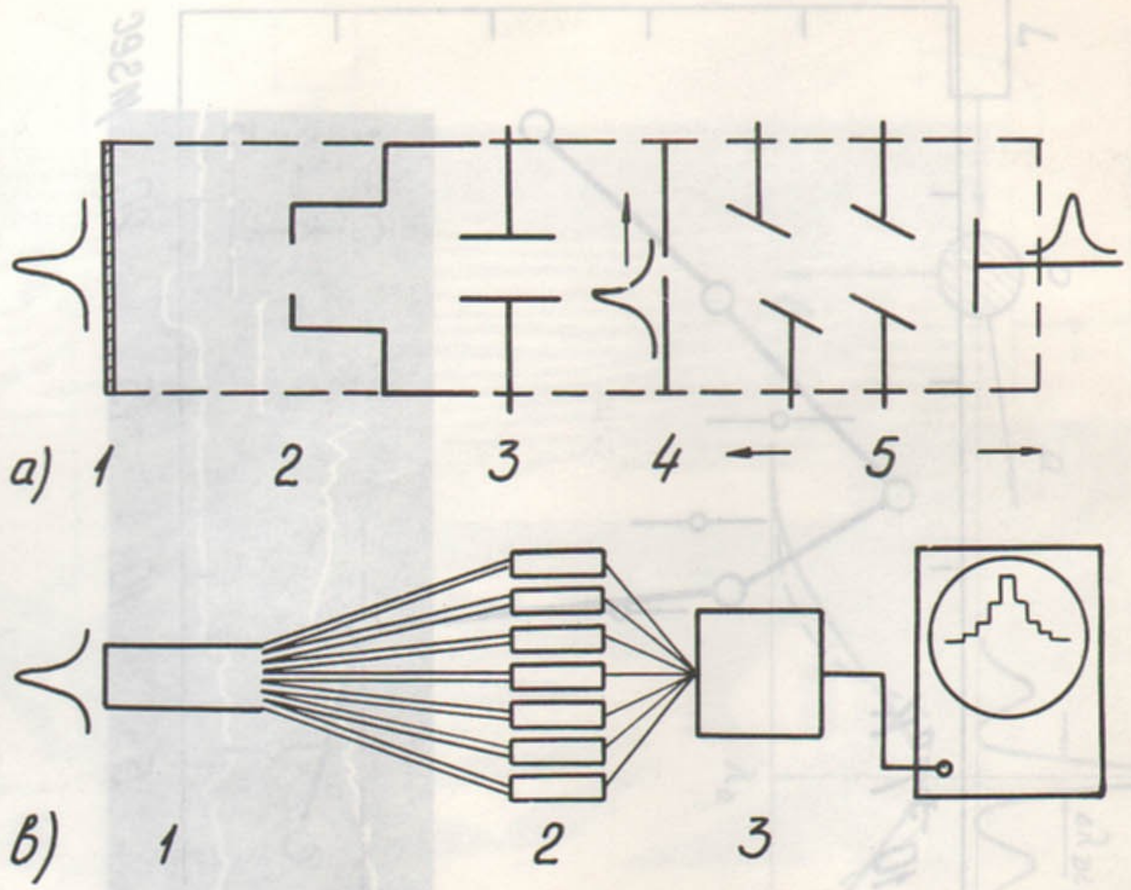

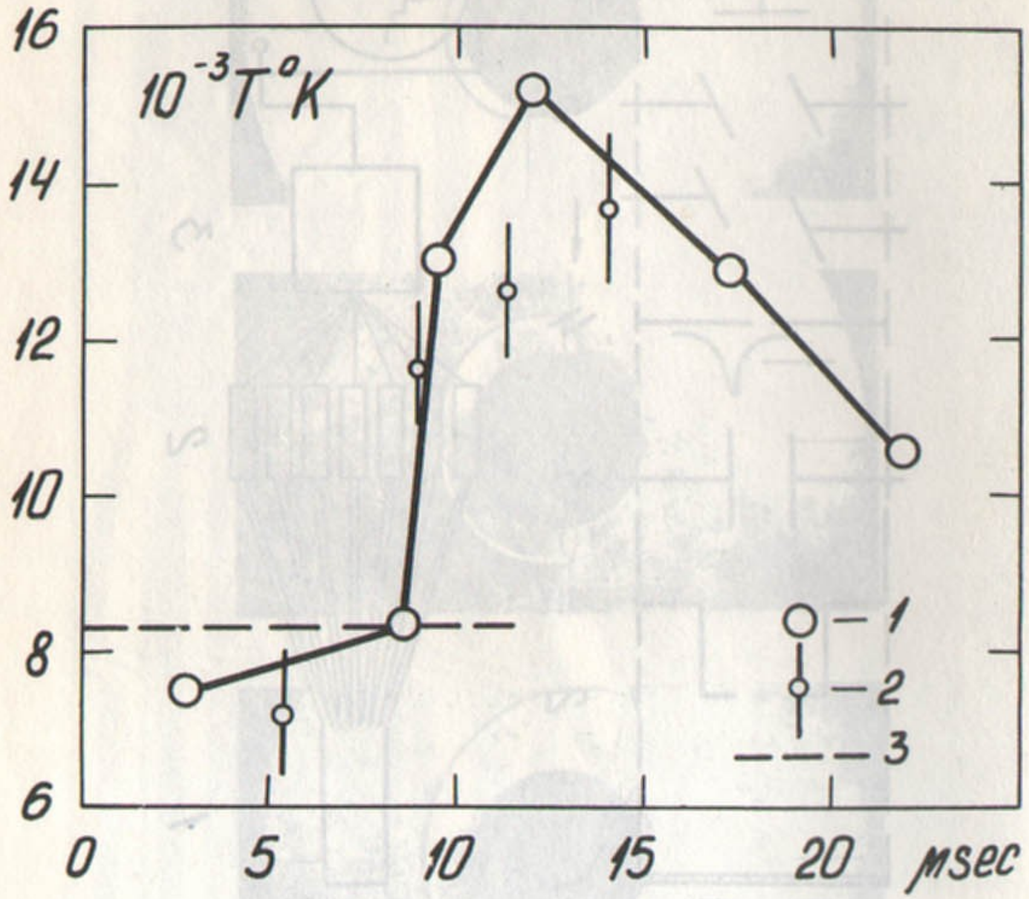

Fig.6

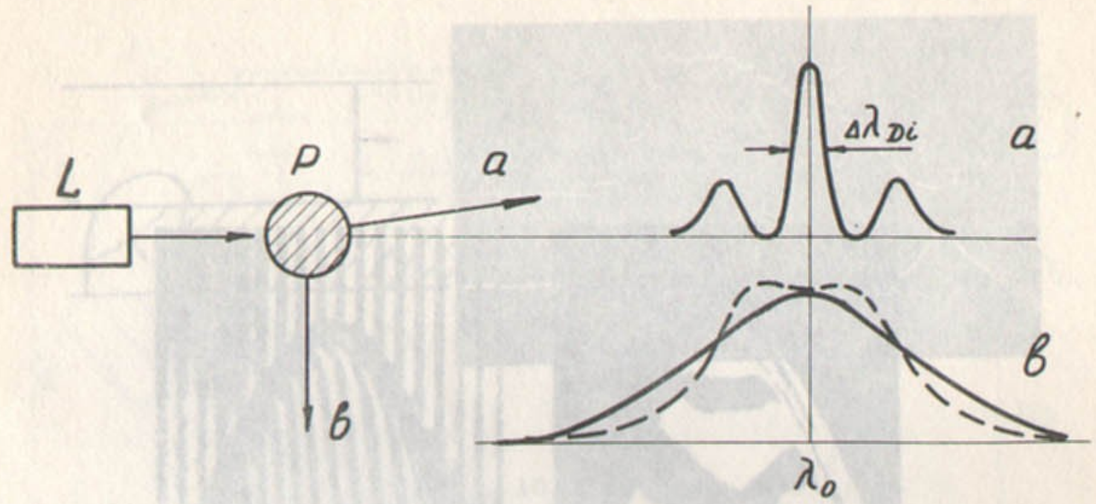

Fig.7

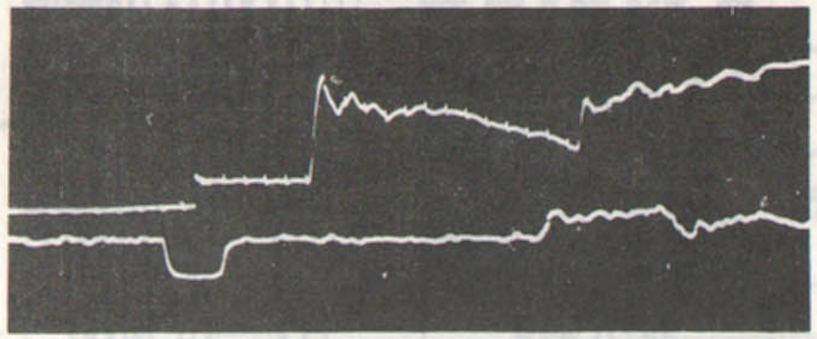

Fig.8

Fig.9

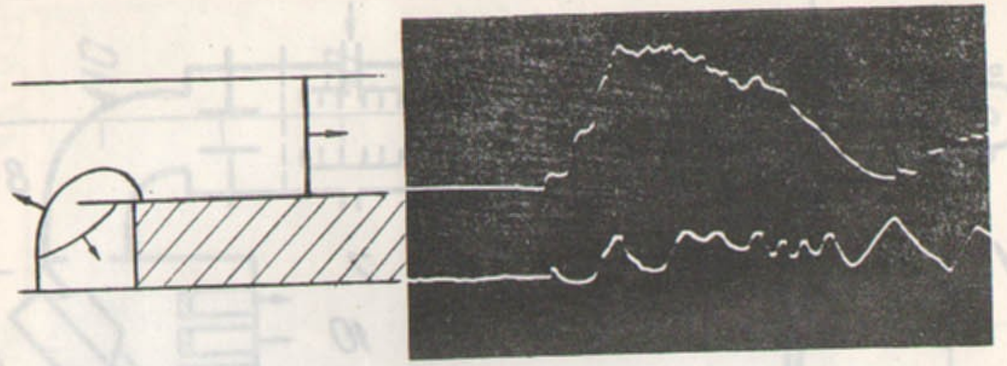

Fig. 10

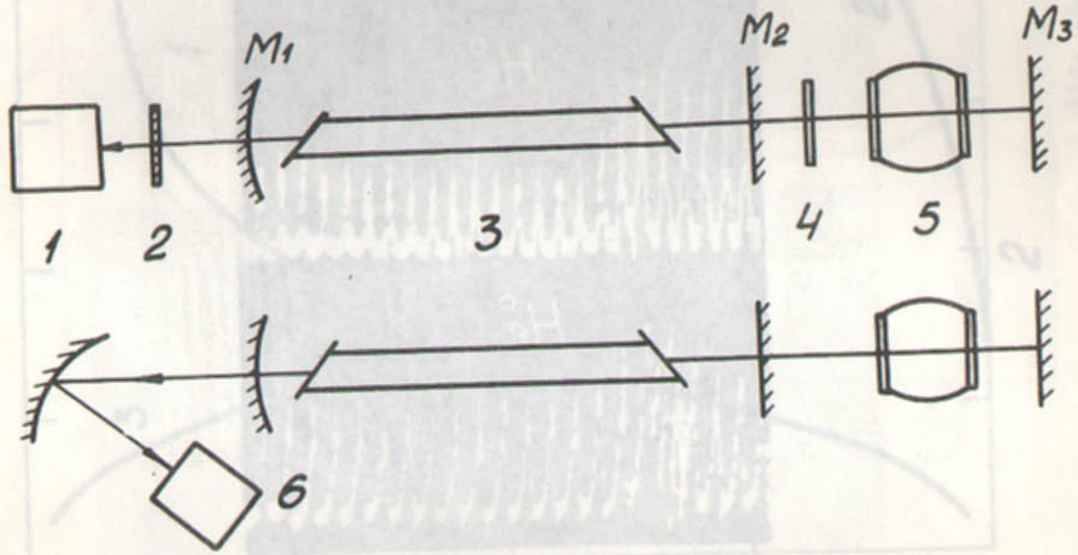

Fig.11

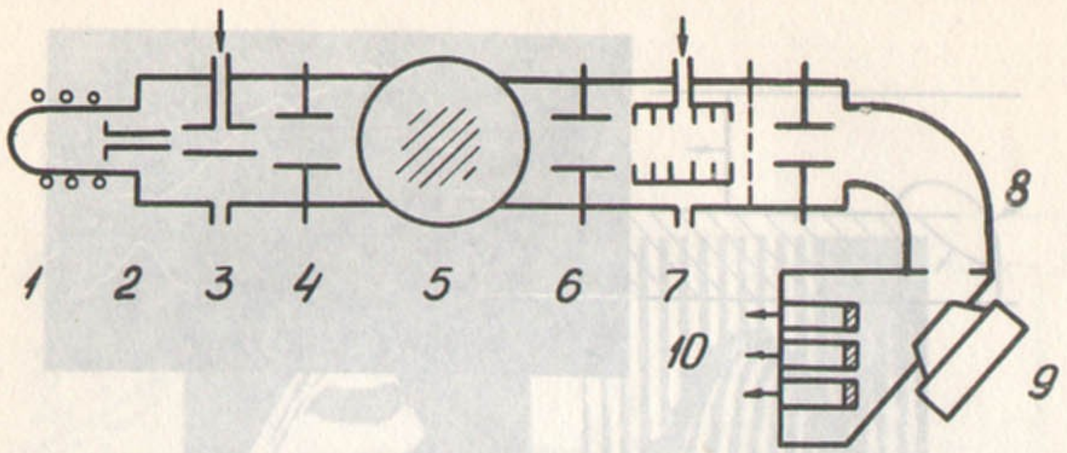

Fig. 12

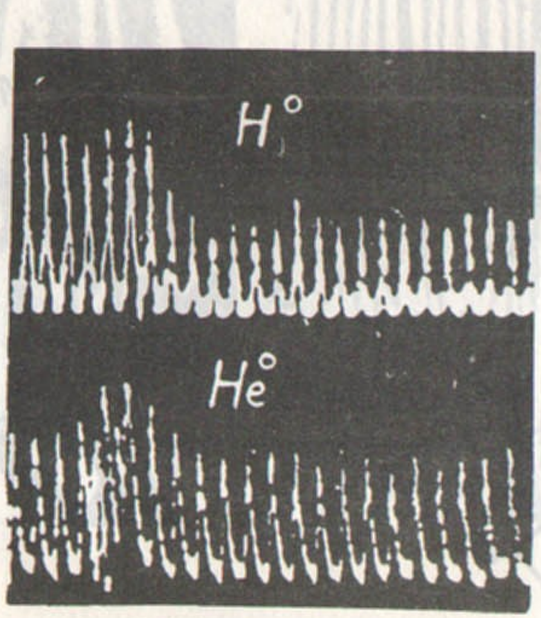

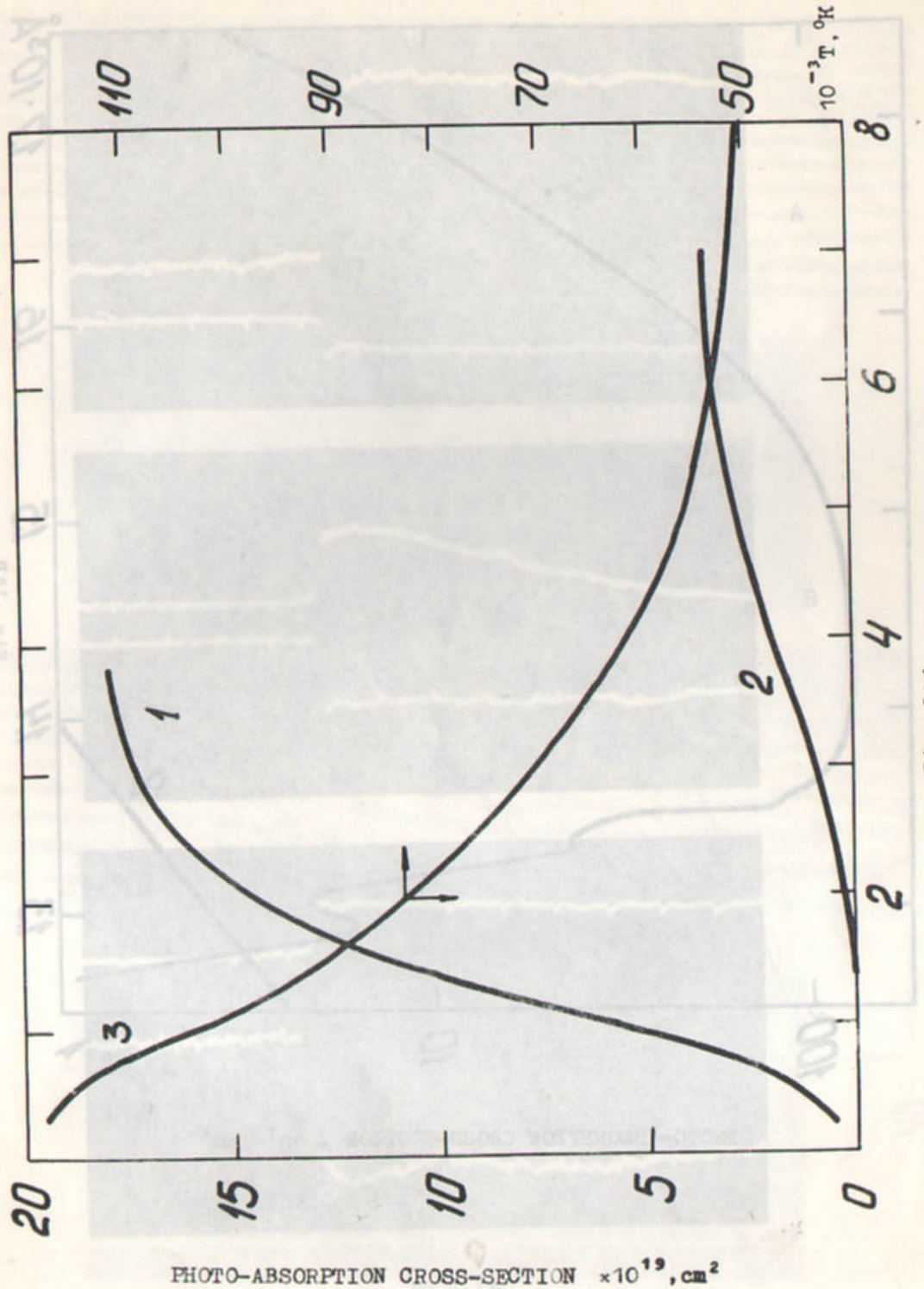

Fig. 14A

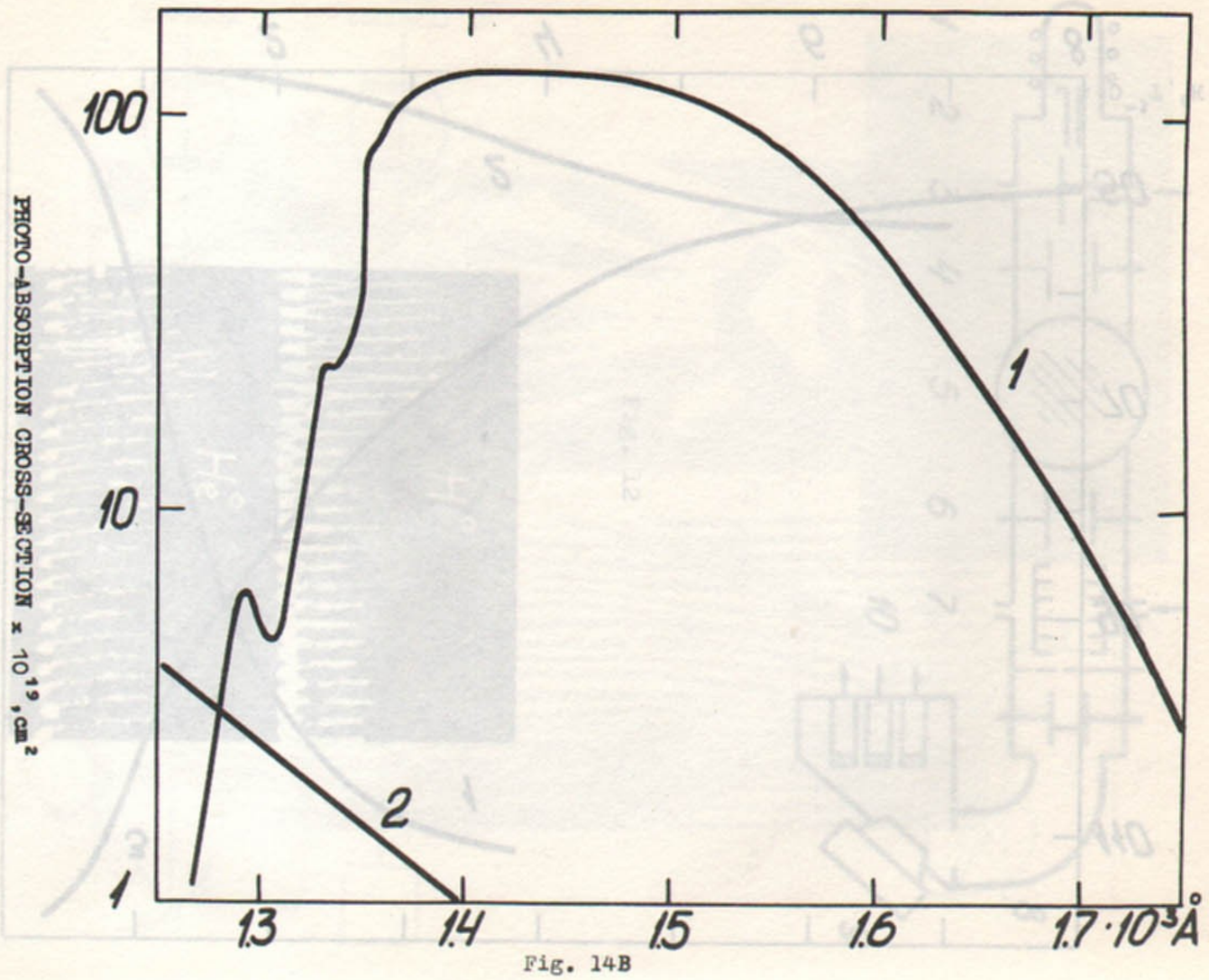

Fig. 14B

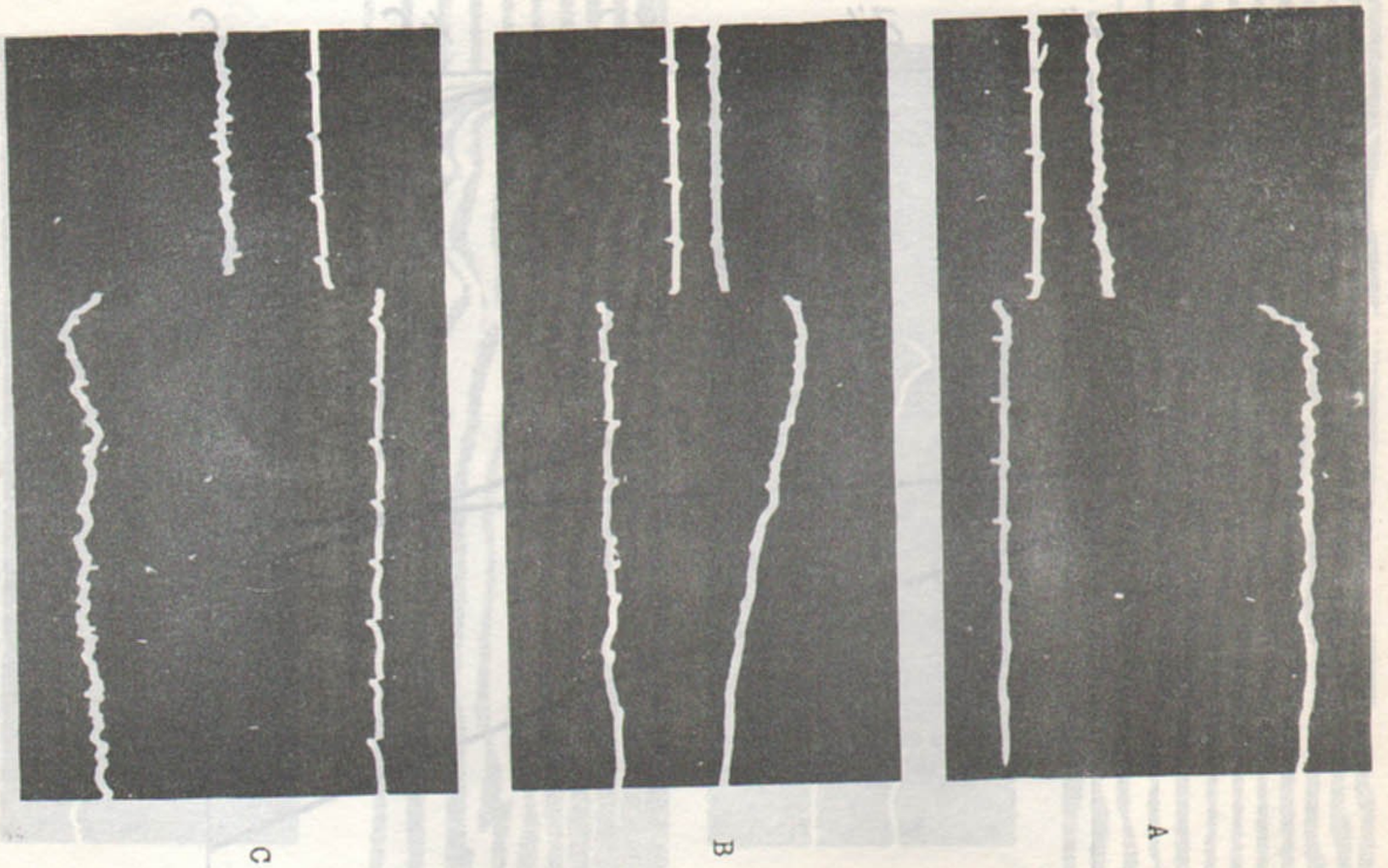

Fig.15

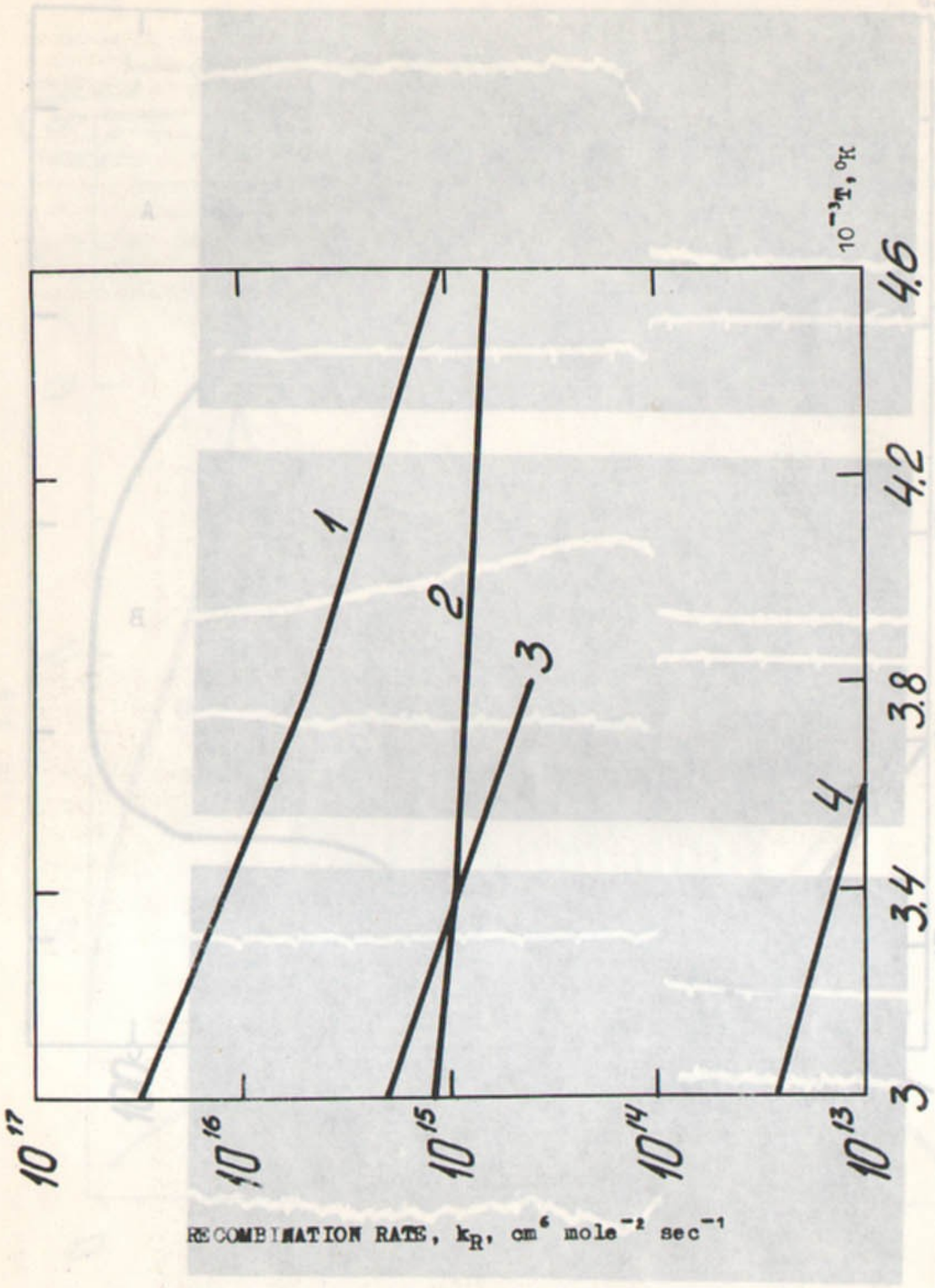
$10^{-3}T$, °K
4.6
4.2
3.8
3.4
3
1
2
3
4
10^{17}
10^{16}
10^{15}
10^{14}
10^{13}
RECOMBINATION RATE, k_R, cm^6 mole^{-2} sec^{-1}

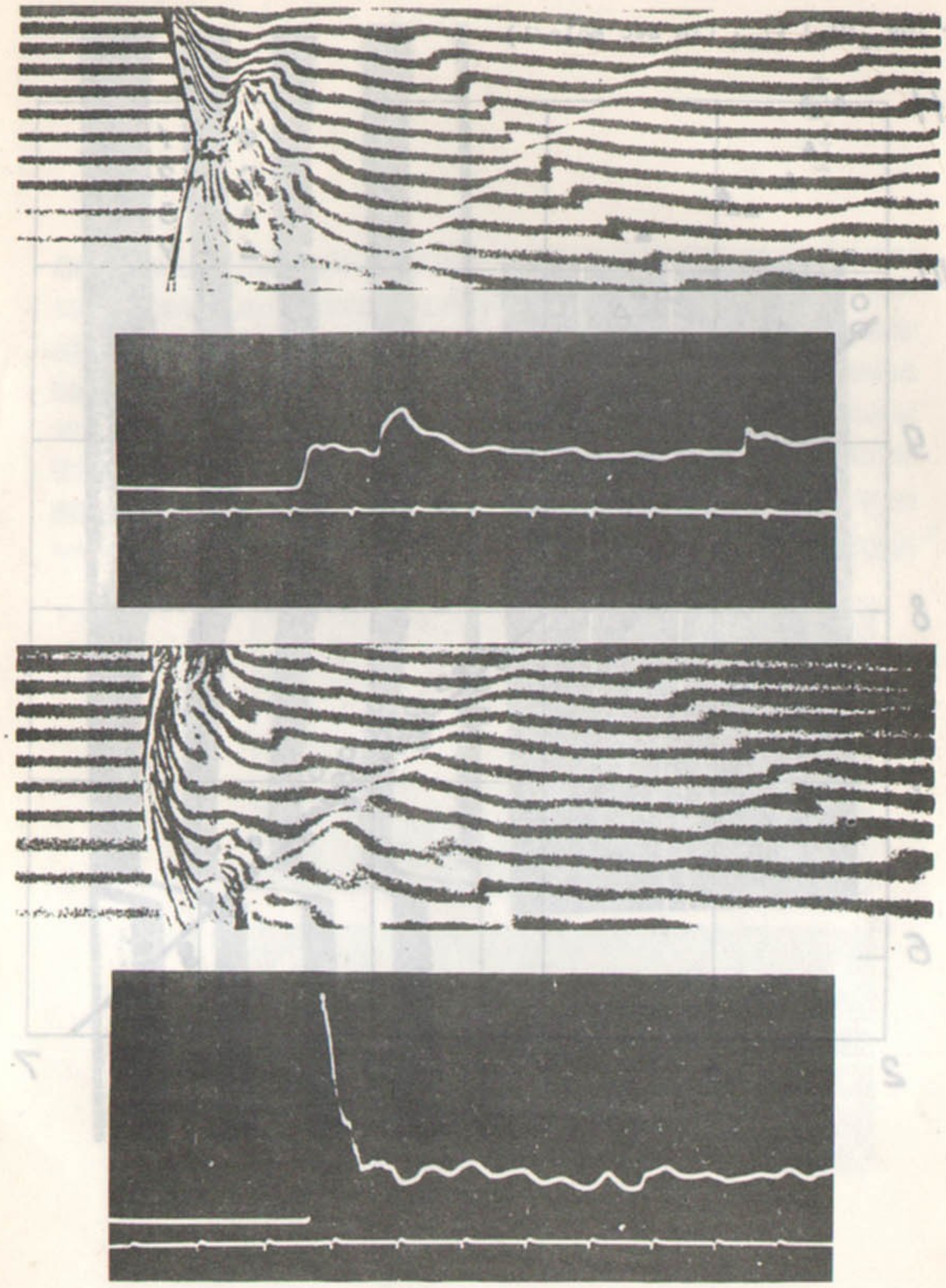

Fig.17

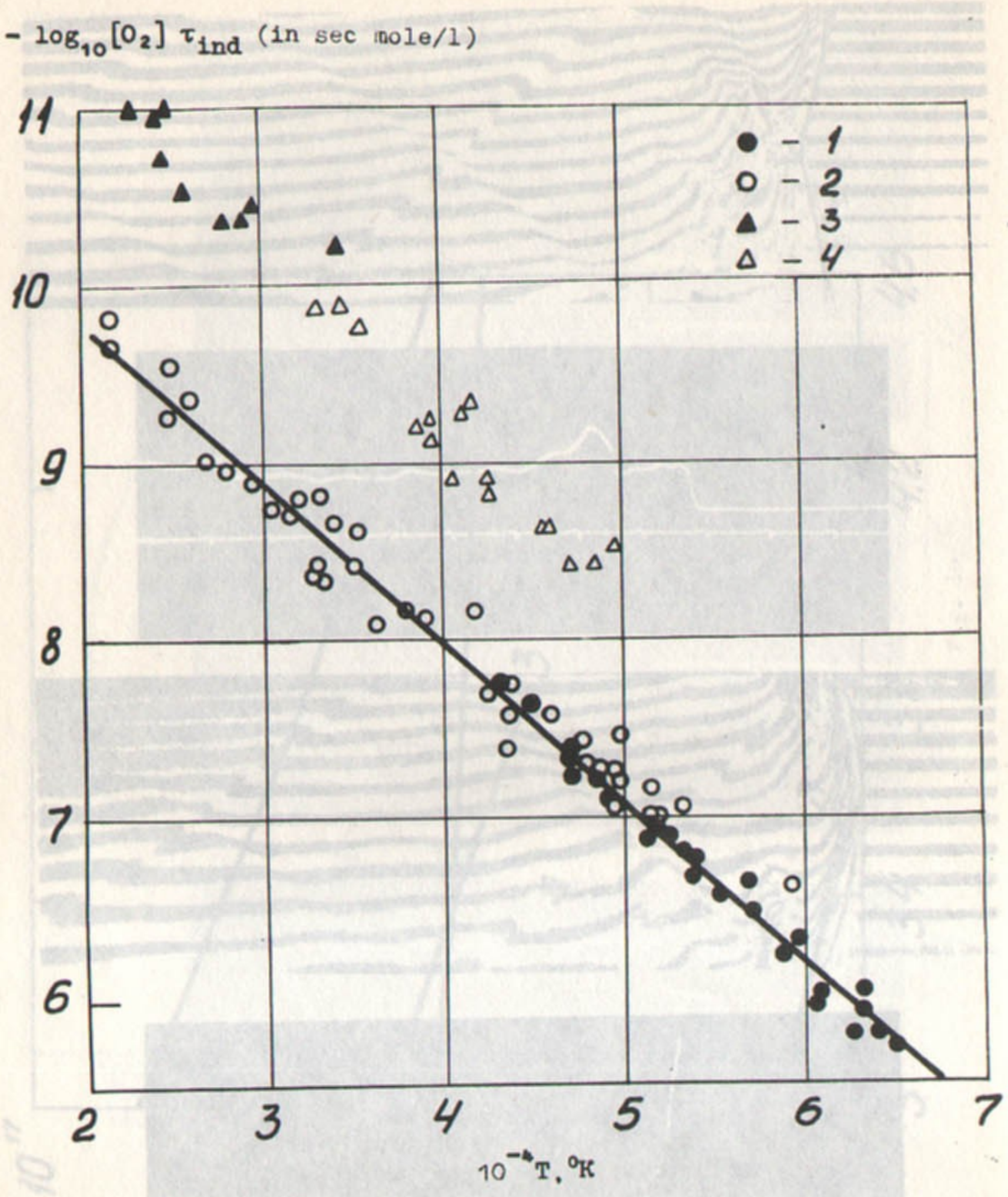

Fig. 18

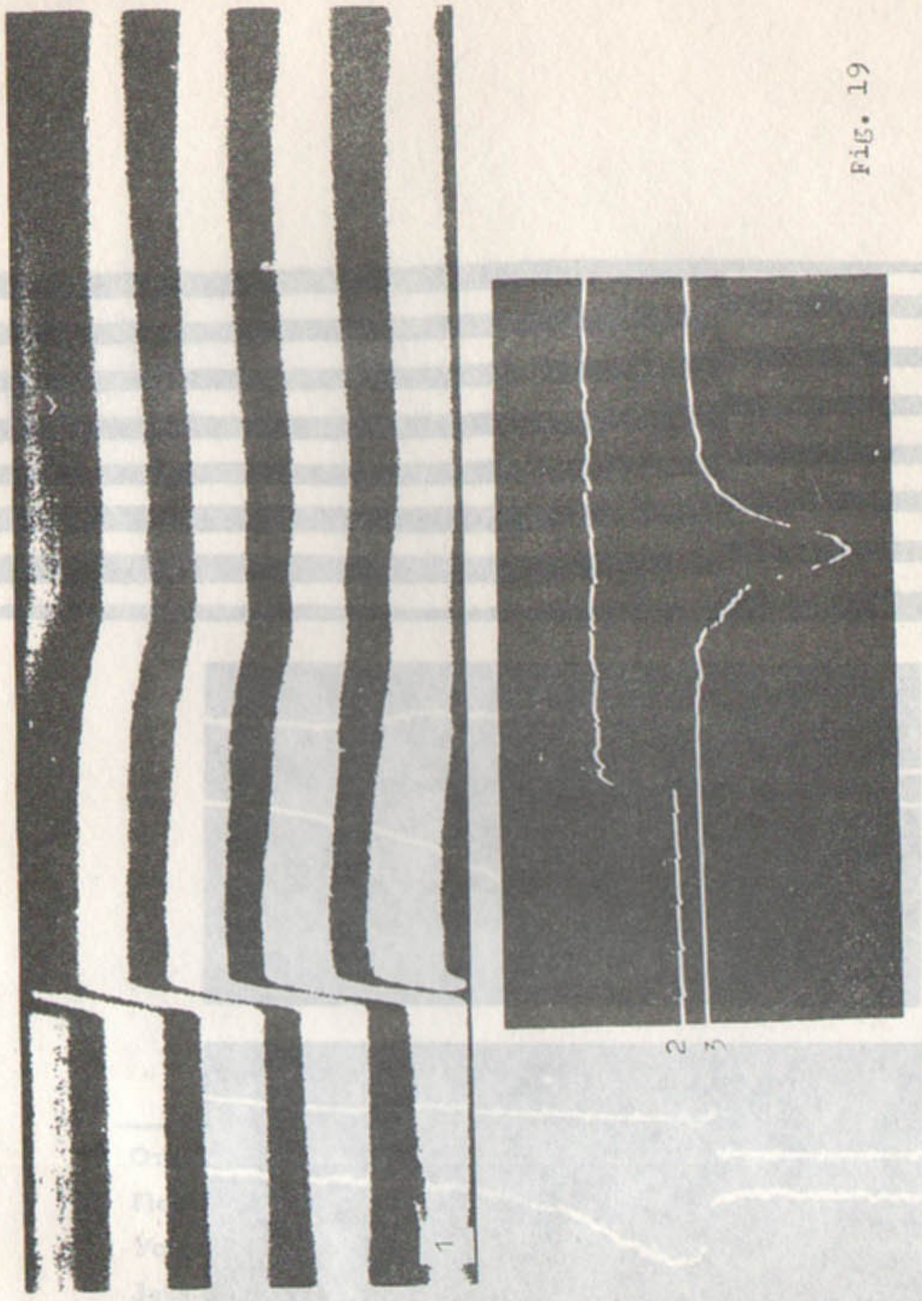

Fig. 19

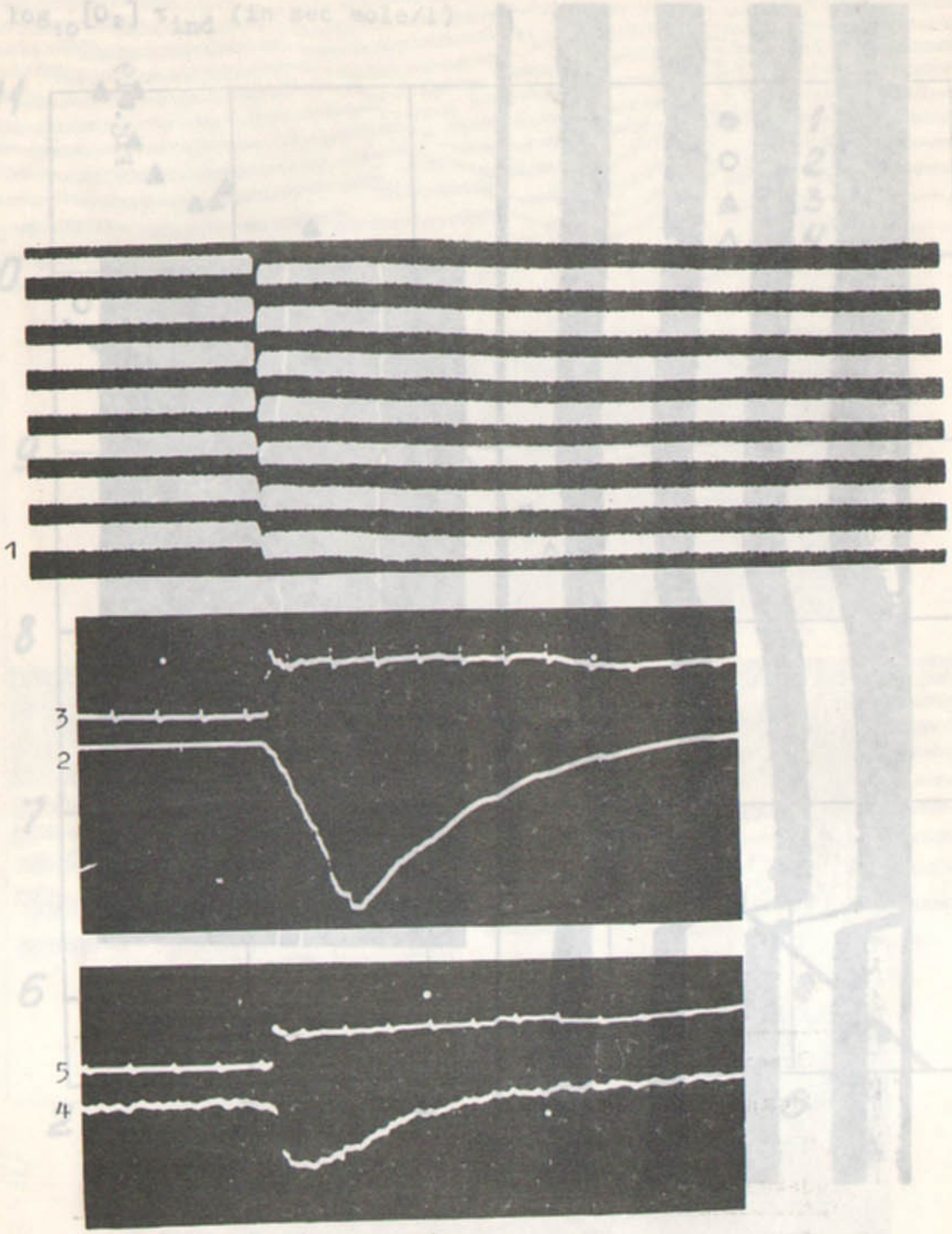

Fig. 20

Ответственный за выпуск Р.И.Солоухин

Подписано к печати 26.5.1969г.

Усл. 3,5 печ.л.. тираж 150 экз.

Заказ № 307. Бесплатно.

Отпечатано на ротапринте в ИЯФ СО АН СССР.